激光与光电子学进展

激光调控优化贵金属复合构型及光激发应用研究进展

徐林林，田悦，焦安欣，陈明*，陈峰**

山东大学物理学院，晶体材料国家重点实验室，山东 济南 250100

摘要 近年来，激光调控优化贵金属纳米复合构型作为一种基于光子与物质相互作用的激发机制的新策略，既可以有效构建出表面洁净无污染的多功能化纳米材料，又能获得常规合成方式难以实现的亚稳相复合构型，因此在众多前沿应用领域具有显著优势。在简单的液相环境中，该策略主要通过聚焦高功率脉冲激光束烧蚀靶材产生高温高压的金属等离子体，后续金属等离子体在热力学非平衡状态下瞬间冷却并成核结晶，从而构建出多种新颖纳米复合构型。此外，该策略充分利用短波长激光束的高光子能量，还可以激发基底材料产生热电子作为独特的还原剂实现周围溶液中金属离子的还原，最终在前驱体负载生长出多形态的金属纳米构型。通过调控激光液相辐照参数，可以有效调控优化贵金属纳米复合构型表面原子的微观形态，使其具备优异的光激发性能，进而被广泛应用于表面增强拉曼散射、光催化、近红外强吸收等应用领域。从激光诱导调控优化金属基纳米复合材料出发，归纳了激光液相诱导策略的可控合成机理，并对激光调控优化贵金属复合构型的潜在应用及未来发展趋势进行了展望。

关键词 激光光学；等离子体；光化学；纳米材料

中图分类号 O436 **文献标志码** A **doi**：10.3788/LOP202158.0700001

Research Progress in Laser-Controlled Optimization of Noble Metal Nanocomposite Configuration and Light Excitation Application

Xu Linlin, Tian Yue, Jiao Anxin, Chen Ming*, Chen Feng**

School of Physics, State Key Laboratory of Crystal Materials, Shandong University, Jinan, Shandong 250100, *China*

Abstract In recent years, as a novel strategy based on the excitation mechanism of photon-matter interaction, laser-controlled optimization of noble metal nanocomposite configuration can not only effectively construct multifunctional nanomaterials with clean surface, but also obtain metastable phase composite configuration which is difficult to achieve by conventional synthesis methods. Therefore, it has significant advantages in many frontier applications. In a simple liquid phase environment, this strategy mainly generates high-temperature and high-pressure metal plasma by focusing a high-power pulsed laser beam to ablate target materials, and then instantaneously cools and nucleates under the thermodynamic non-equilibrium state, thereby constructing various unique nanostructures. In addition, making full use of the high photon energy of the short wavelength laser beam, this strategy can also excite the substrate material to produce hot electrons, which can be used as a unique reducing agent to realize the reduction of metal ions in the surrounding solution, and finally grows multi-morphology metal nanostructures on the precursor. By adjusting the laser liquid phase irradiation parameters, the surface atom microscopic morphology of the optimized noble metal nanocomposite configuration can be effectively adjusted to make it have excellent light excitation

收稿日期：2020-09-14；**修回日期**：2020-11-02；**录用日期**：2020-11-18

基金项目：国家自然科学基金(11575102)

E-mail**：chenming@sdu.edu.cn；*E-mail**：drfchen@sdu.edu.cn

performance, and then it is widely used in surface enhanced Raman scattering, photocatalysis, near infrared strong absorption, and other application areas. In this paper, the controllable synthesis mechanism of the laser-induced liquid-phase strategy is summarized based on laser-induced optimization of metal matrix nanocomposites, and the potential applications and future development trend of laser-controlled optimization of noble metal composite configurations are prospected.

Key words laser optics; plasma; photochemistry; nanomaterials

OCIS codes 140.3390; 250.5430; 350.5130; 160.4236

1 引　　言

近年来，通过引入贵金属元素构建的新型复合纳米材料具备独特的可调谐电子微观结构，展现了极为优异的光-电转化/传输特性，极具应用潜力，在生物医学、环境监测、食品安全、能源转化/存储、催化等众多领域发挥着重要作用[1-6]。贵金属复合纳米材料的结构组分、微观形态以及界面构型的优化设计是不断提高其光/电性能的至关重要环节，进而促进后续的前沿交叉应用研究。为实现贵金属复合构型的微观精细调控，尤其是在空心笼状、核壳多层、长枝状等众多复杂结构制备中，常规合成方式如模板法、水热法、沉淀法、溶胶-凝胶法、微乳液法、电解法等通常需要借助复杂、多样的封端试剂作为金属原子成核结晶的保护配体，以此控制纳米金属的生长方式[7-10]。后续附着于纳米产物表面的有机试剂所形成的隔离层将会降低光-电转化/传输性能，因此还必须通过繁琐严苛的清洗-提纯等工艺对材料表面进行除杂净化。研究人员不断优化常规合成方式以期减少使用辅助试剂，同时更加迫切需要探索一种绿色环保的新颖调控策略，为获得表面洁净无污染的贵金属纳米复合构型开辟新思路。基于此，激光调控优化策略应运而生。

激光调控优化策略是基于光与物质相互作用的激发机制，通过光子在材料中的吸收-转化-激发，实现对于材料结构改性的微加工设计。尤其是在液相环境中，通过激光辐照可以对金属材料进行高效激发，产生一系列新颖的物理化学反应，据此能够实现独特的金属原子成核-结晶-生长，其显著优势在于可以有效弥补传统微加工过程中固有的工艺复杂、周期长、易引入杂质等不足[11-16]。其中，经过聚焦脉冲激光束烧蚀靶材产生的高温高压等离子体可以在液相环境中瞬间冷却并成核结晶，该过程无需外界提供辅助生长试剂，通过调节激光参数有效调控金属纳米复合材料的组分与形貌，更为重要的是可以通过这种热力学非平衡状态的独特纳米材料生长方式获得常规化学反应中难以形成的亚稳相复合构型[17-22]；此外，基于短波长激光束（尤其是紫外光）液相辐照方式，被吸收的高能量光子可以有效激发基底材料产生热电子，由此构成的新颖还原剂能够对周围溶液中的金属离子实现高效、原位还原，进而在基底材料表面负载生长出多形态的纳米金属复合构型[23-27]。总之，利用激光束来诱导驱动液相反应可以作为金属纳米复合材料的调控合成策略，通过合理控制激光辐照参数还能够对所构建的微观结构表面原子进行系统的优化设计。

本文简明扼要地对激光液相作用的方式与原理进行了综述，并对其优化设计的多种贵金属复合材料的表面增强拉曼散射的光激发特性进行了较为详细的探究。综述了近几年利用脉冲激光聚焦烧蚀技术以及连续激光液相辐照技术合成的多种奇特的金属复合构型。此外，基于上述讨论，进一步归纳了金属基复合构型在其他光激发领域的应用价值，如光催化、近红外吸收等。

2 基于脉冲激光聚焦烧蚀调控优化贵金属复合构型

利用聚焦脉冲激光束在液相环境中烧蚀贵金属固体靶材，基于高功率激光与物质的相互作用诱导产生高温高压的金属等离子体，金属等离子体在液相中急剧冷却并成核结晶，实现多形态纳米复合材料的构建，通过调节激光作用参数还能够有效优化微观构型，进而为后续探索其优异的物理/化学性能奠定基础。在将高功率激光束作为激发源用于调控优化贵金属纳米复合构型的研究过程中，科研人员多年来一直致力于探索激光与物质相互作用的内在机理，以此阐明激光液相烧蚀（LAL）过程中的主要物理/化学过程，这将为深入研究金属纳米复合材料的可控合成机制提供丰富的理论/实验依据[28-32]。在此总结了前期主要的研究工作，对基于脉冲激光液相烧蚀构建多种纳米结构的过程中涉及的物理化学机理进行综合探讨。根据不同脉

宽激光与固体靶材作用机理的不同，从短脉宽（纳秒、皮秒、飞秒）和长脉宽（毫秒）脉冲激光液相烧蚀两部分进行简单的归纳总结。

2.1　脉冲激光液相烧蚀机理

短脉宽脉冲激光液相烧蚀的主要物理/化学过程随着时间演化可以归纳为等离子体的产生、膨胀、湮灭三个阶段，如图 1(a)～(e)所示[33]。第一阶段为等离子体的产生[图 1(a)]：当聚焦脉冲激光束通过液相环境到达固体靶材表面之后，短脉宽激光束中具有高功率密度的超快光子作用到靶材，在聚焦斑点处进行瞬间的激发烧蚀。被烧蚀靶材在极短脉冲瞬间（10^{-12}～10^{-10} s）快速被加热至熔化甚至汽化，产生的气体与激光进一步作用，绝大部分发生电离，进而形成由靶材原子、自由电子、离子等组成的高密度等离子体。第二阶段为等离子体的膨胀[图 1(b)、(c)]：周围液相条件的限制作用决定了等离子体后续的膨胀过程可以产生几千 K 的温度和几十 GPa 的压力，尤其是飞秒脉冲激光液相烧蚀法，其在脉冲激光聚焦区域的温度高达 10000 K 以上，压强也在 20 GPa 以上[34-35]。这一高温高压等离子体在随后膨胀的过程中会与周围液相环境直接作用，发生众多化学反应，这为调控和构建金属纳米复合材料提供了理想的反应环境。第三阶段为等离子体的湮灭[图 1(d)、(e)]：待脉冲结束后，由于等离子体不能进一步吸收激光能量，其高温高压的状态不能继续维持，最终在湮灭冷凝过程中成核、生长形成纳米颗粒。图 1(f)展示了激光液相烧蚀的三个主要阶段及与之相对应的实时照片，直观地阐述了等离子体在液相环境中的物理/化学变化过程。此外，通过成像技术，科研人员多次拍摄到激光液相烧蚀过程中等离子体的形成、膨胀、湮灭过程，这进一步证实了上述机理[36-39]。如图 1(g)所示，Yang 等[40-42]通过纳秒拍照设备研究了激光液相烧蚀铂丝的机理，清晰地揭示了等离子体的膨胀和湮灭过程。值得注意的是，该过程中金属等离子体的冷却过程极为短暂，并伴随着周围介质的收缩和汽化。相比于应用较为广泛的纳秒脉冲激光，飞秒脉冲激光束由于具有超短脉冲宽度，极大地提高了激光的峰值强度，使其烧蚀过程中辐照焦点的温度得以明显提高，这种独特的烧蚀过程更有利于诱导

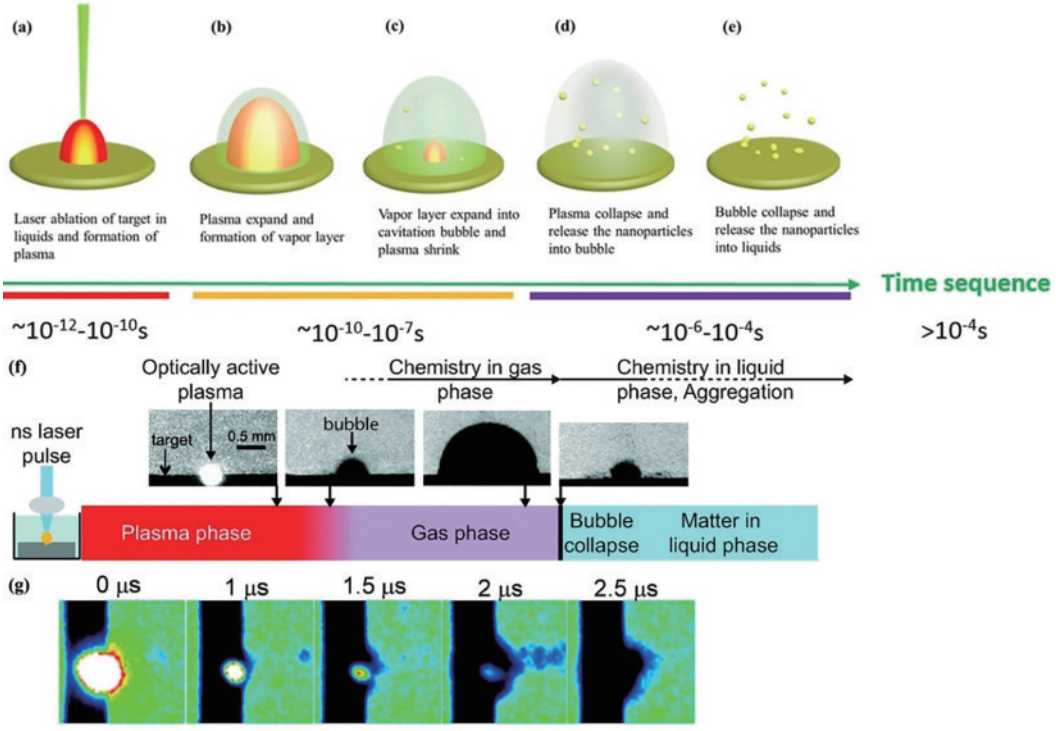

图 1　脉冲激光液相烧蚀的主要机制。(a)～(e)脉冲激光液相烧蚀随时间的演化过程（以纳秒脉冲激光为例）[31]；(f)激光-靶材-液体系统在每个激光脉冲期间发生的主要阶段及与之对应的实时图片[33]；(g)脉冲激光烧蚀水中铂丝时诱导的等离子体和空化气泡分布图[36]

Fig. 1　Main mechanism of pulse laser ablation in liquid solution. (a)-(e) Evolution of pulsed laser ablation in liquid solution with time (take nanosecond pulse laser as example)[31]; (f) main stages and their corresponding real-time images of laser-target-liquid system for each laser pulse[33]; (g) laser-induced plasma and cavitation bubbles on Pt wire in water[36]

形成极为显著的高温高压等离子体，可以调控、制备出常规合成方式难以实现的更为新颖的纳米微观结构。

上述过程中提到，脉冲激光烧蚀金属靶材形成的等离子体在膨胀过程中，在等离子体内部、液体内部、等离子体与液相介质的界面处存在反应团簇，由此可以诱导 4 种化学反应，如图 2 所示。如图 2(a)所示，第一种化学反应发生在激光诱导的等离子体内部。由于激光诱导的高密度等离子体处于高温高压状态，该过程将会形成常规方法无法获得的亚稳相材料。具有代表性的研究工作主要包括六方碳相到立方碳相的转变以及闪锌矿硅相转变为面心立方硅相[43-46]。如图 2(b)所示，第二种化学反应也发生在激光诱导的等离子体内部。脉冲激光烧蚀金属靶材产生的等离子体会导致不同液体的界面处液体分子的激发和蒸发，并在等离子体-液体界面处产生新的等离子体。该处的等离子体一旦产生，两种等离子体会迅速碰撞并混合，进而发生化学反应。具有代表性的化学反应过程是各种氧化物、氮化物和碳化物的形成过程[47-49]。如图 2(c)所示，第三类化学反应发生在激光诱导的等离子体与液体之间的界面处。激光诱导的高温、高压、高密度等离子体能够与液相分子发生高温化学反应。具有代表性的化学反应过程为激光液相烧蚀过程中水合氧化物的产生过程[50-51]。如图 2(d)所示，第四类化学反应发生在液体内部。来自固体靶材的烧蚀物质将在极强的作用力下从激光诱导的等离子体中喷溅到液体中，此时烧蚀物质与液体分子之间的化学反应将发生在液体内部，具有代表性的化学反应过程主要是氢氧化物的形成过程[52]。由此可见，通过改变烧蚀过程中的激光参数(波长、脉宽、能量、频率、作用时间、光斑面积)和材料参数(固体靶材、溶剂/质、系统温度和压力)能够完成多种贵金属复合构型的优化设计。

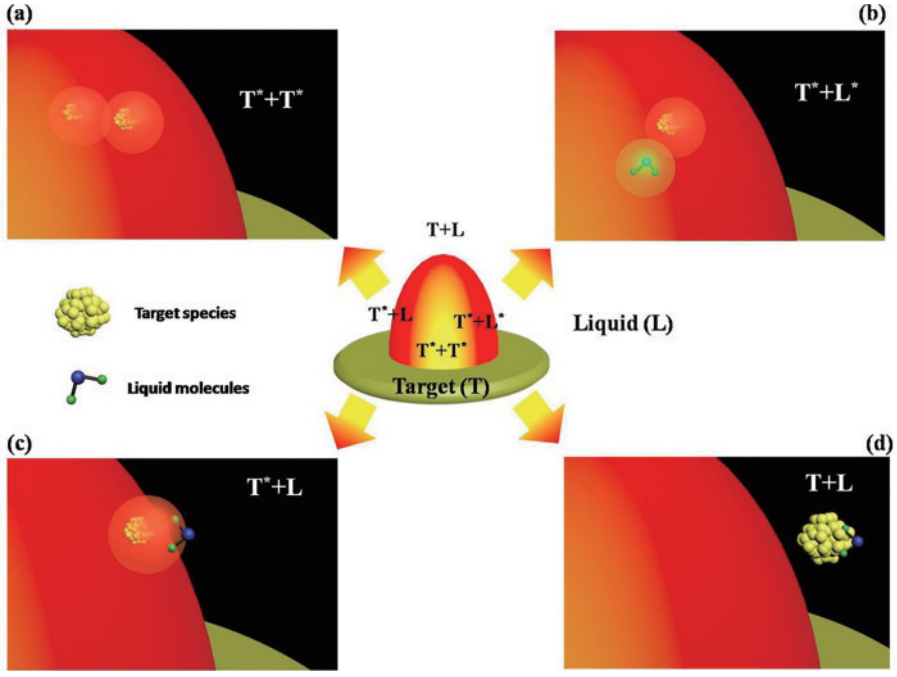

图 2　在等离子体、液体内部以及等离子体和液体之间的界面处发生的 4 个化学反应[31]。(a)在激光诱导的等离子体内部，反应团簇为靶材等离子体；(b)在激光诱导的等离子体内部，反应团簇为靶材等离子体和液体分子；(c)在激光诱导的等离子体和液体之间的界面上，反应团簇为靶材等离子体和液体分子；(d)在液体内部，反应团簇为靶材和液体分子

Fig. 2　Four chemical reactions occur inside the plasma and liquid and at the interface between the plasma and the liquid[31]. (a) In the laser-induced plasma, reaction clusters are target plasma; (b) in the laser-induced plasma, reaction clusters are target plasma and liquid molecules; (c) at the interface between laser-induced plasma and the liquid, reaction clusters are target plasma and molecules of the liquids; (d) in the liquid, reaction clusters are the target and molecules of liquid

早期的研究中，与短脉宽激光相比，毫秒脉冲激光很少用于纳米材料的合成，更多的是用于焊接和切割金属[53]。2010 年，天津大学 Niu 等[54]系统地探究了毫秒激光液相烧蚀过程中各种参数(激光频率、激光能量、脉冲宽度、金属靶材、液相介质)对纳米产物的微观调控，首次提出并验证了毫秒脉冲激光烧蚀

喷射的金属液滴的表面反应进程直接决定了产物的最终结构，如图3所示。基于毫秒脉冲激光低功率密度的特点（10^6～10^7 W/cm^2），加热效应是调控纳米材料微观结构的主要机制。在这一过程中，激光在液相介质中烧蚀固体靶材时，如图3(a)所示，光斑的作用区域会发生熔化，产生温度很高的毫米级金属液滴，以至于其周围的液体介质被汽化并且液体层的限制作用导致产生高压蒸汽；随后，这一高压蒸汽会产生很强的粉碎效应，使得最初的毫米级液滴爆炸性地溅射出大量的纳米液滴；金属纳米液滴有望与周围液体介质发生表面反应[图3(b)]形成纳米材料。上述理论已经通过高速条纹相机拍摄的毫秒激光烧蚀水中钛靶的实时图片得到进一步证实，如图3(c)所示。从0.2～2.2 ms的时间分辨图像可以清晰观察到大量纳米金属液滴的存在，同时并未出现图1(f)所示的半球状的等离子体羽区。本工作以Pb/S反应体系为例，通过精确地调控激光频率和液体介质反应活性，优化设计出空心、核壳、异质结、纳米立方体、纳米管等多种形貌的Pb/S金属复合材料。此外，相关扩展研究工作还进一步探索了Mg/O、Zn/S等体系的反应过程，为后续的毫秒脉冲激光液相烧蚀研究提供了依据。

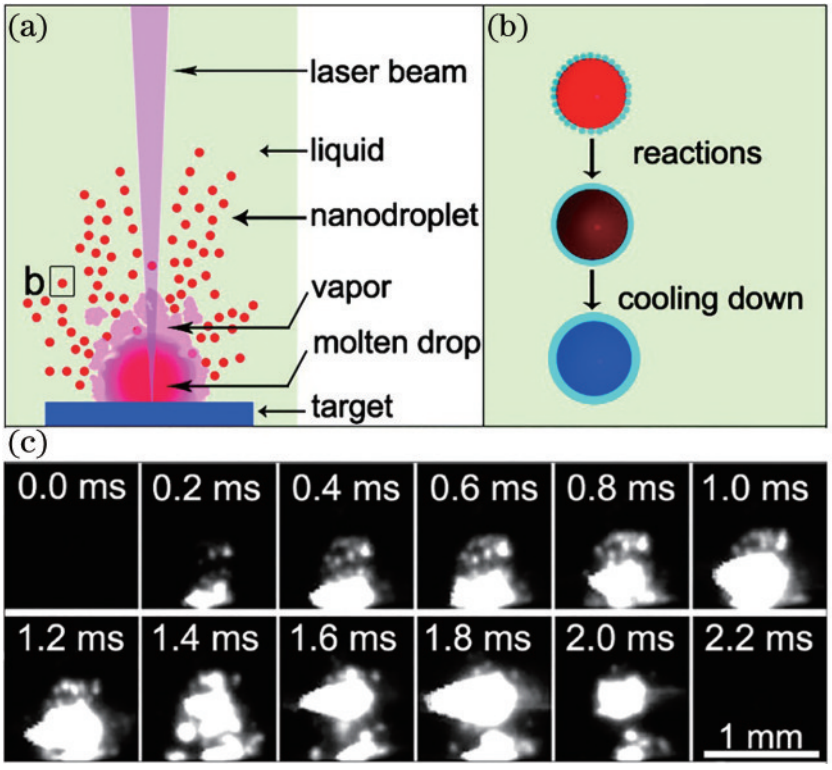

图3　毫秒脉冲激光液相烧蚀机制[54]。(a)纳米液滴的形成；(b)溅射出来的金属纳米液滴与周围的液体介质反应；(c)激光烧蚀水中钛靶的实时图片

Fig. 3　Mechanism for ms pulsed laser ablation in liquid[54]. (a) Formation of nanodroplets; (b) reaction of ejected metal

本节简要归纳了短脉宽（纳秒、皮秒、飞秒）和长脉宽（毫秒）脉冲激光液相烧蚀过程中发生的独特物理化学现象。众多研究结果表明，当使用不同脉冲宽度的激光作用液相金属靶材时，金属纳米复合构型的调控合成机理有所不同：短脉宽激光液相烧蚀主要基于高温高压等离子体的产生、膨胀和湮灭，最终等离子体凝聚、成核、生长形成纳米材料；长脉宽激光液相烧蚀的微观结构调控则取决于加热效应形成的纳米液滴的表面反应。由于其烧蚀过程的明显差异性，短脉宽/长脉宽激光液相烧蚀均具有各自的优点和与之相关的应用领域。由此可见，全面了解激光液相烧蚀的基本机理有利于调控、设计出具有特定功能的金属基复合纳米结构。

2.2　基于脉冲激光液相烧蚀策略优化设计金属复合构型

基于激光液相烧蚀策略，科研人员已经优化设计了多种形貌、组分的高性能纳米结构，包括花状、二维片状、单分散球状、纤维状、管状、海胆状、棒状、

立方体等多种形貌的金属、氧化物、氮化物、硫化物、合金、多金属氧酸盐等[55-66]，如图 4 所示。除了可以实现多形貌、多组分的优化调控以外，激光液相烧蚀技术最大的优势在于：利用该合成方式的瞬间高温高压和快速淬火的特点，可以制备出常规合成条件下难以形成的亚稳相材料[17-22]。作为一种介于稳定相和非稳定相的中间状态，亚稳相可视为相变系统发生质变和量变的过渡区，即系统处于非平衡状态的一种表现形式。亚稳相材料既可以作为结构材料，也可以作为功能材料应用于不同的场合。同一化学组分的材料，其亚稳相时的性能不同于平衡态时的性能，而且在很多情况下，亚稳相材料的光学、电学、催化等特性远优于稳相材料[67-71]。因此，亚稳相材料也成为人类发现新物质和新的物理化学现象的重要研究材料，具有很大的研究意义和价值。

2015 年，中山大学杨国伟课题组采用激光液相烧蚀策略首次合成了自然界中难以存在的亚稳相白碳（Carbyne）及其凝聚相白碳晶体，如图 5（a）所示[17]。通过选择合适的液体环境和固体靶材，他们巧妙地利用贵金属高温脱氢反应和激光液相烧蚀所提供的高温高压热力学环境，在液相环境中实现了白碳分子的成核与生长，合成出了白色粉末

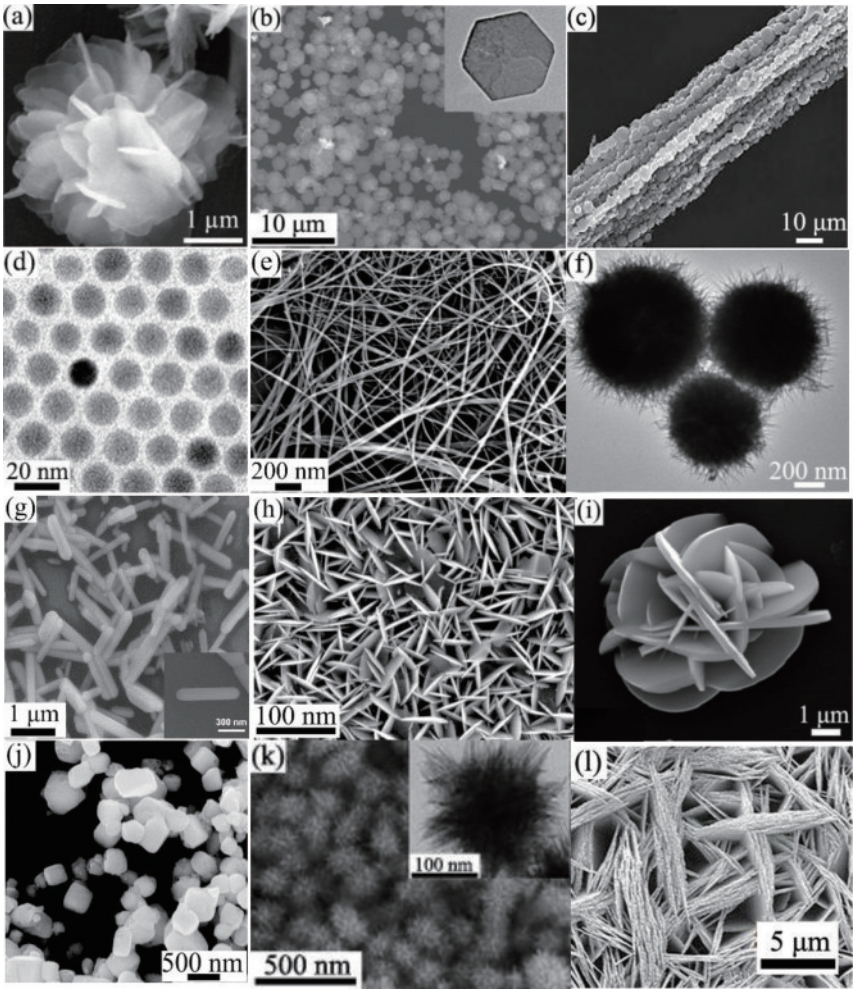

图 4　激光液相烧蚀合成的多种纳米结构的独特形态。（a）氢氧化锌/十二烷基硫酸盐纳米结构[55]；（b）PdO 纳米片[56]；（c）Fe_3C 超细纤维[57]；（d）Cd 单分散量子点[58]；（e）MnOOH 纳米线[59]；（f）板栗状 Fe_3O_4@C@$ZnSnO_3$ 核壳层级结构[60]；（g）$Cu_3Mo_2O_9$ 纳米棒[61]；（h）Ge 掺杂的 α-Fe_2O_3 纳米片[62]；（i）$ZnMoO_4$ 纳米花[63]；（j）AgCl 立方体[64]；（k）海胆状 $ZnSnO_3$[65]；（l）Ag 纳米片[66]

Fig. 4　Distinctive morphologies of nanostructures synthesized by laser liquid phase ablation. (a) Zinc hydroxide/dodecyl sulfate nanostructures[55]; (b) PdO nanosheets[56]; (c) Fe_3C superfine fiber[57]; (d) Cd monodispersed quantum dots[58]; (e) MnOOH nanowires[59]; (f) chestnut-like Fe_3O_4@C@$ZnSnO_3$ core-shell hierarchical structure[60]; (g) $Cu_3Mo_2O_9$ nanorods[61]; (h) Ge-doped α-Fe_2O_3 nanosheet[62]; (i) $ZnMoO_4$ nanoflowers[63]; (j) AgCl cubes[64]; (k) urchin-like $ZnSnO_3$[65]; (l) Ag nanoplates[66]

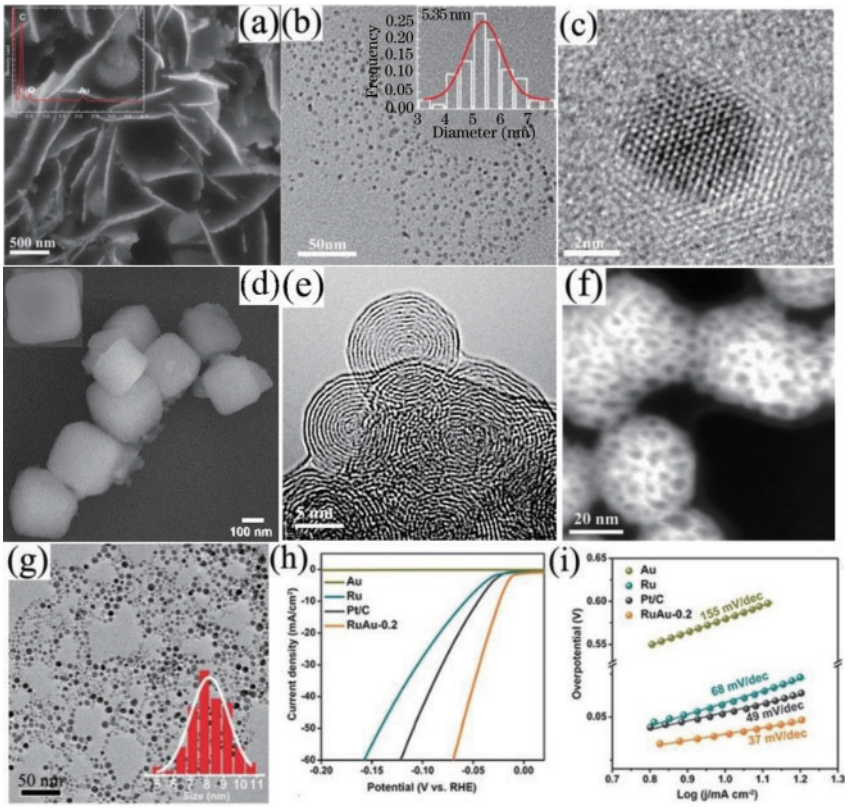

图 5　激光液相烧蚀合成的多种亚稳相结构。(a)白碳[17];(b)(c)纳米金刚石[72];(d)类 C_8 碳纳米立方体[73];(e)碳洋葱[74];(f)面心立方金刚石[74];(g)亚稳相 RuAu;(h)线性扫描曲线;(i)从图 5(h)中得出的塔菲尔斜率[18]

Fig. 5　Various metastable structures synthesized by LAL. (a) Carbine[17]; (b)(c) nanodiamonds[72]; (d) C_8-like carbon nanocubes[73]; (e) carbon onions[74]; (f) fcc new diamonds[74]; (g) metastable RuAu; (h) linear scanning curves; (i) Tafel slopes derived from Fig. 5(h)[18]

状的白碳晶体。此外,如图 5(b)~(f)所示,该研究组还设计出了其他一系列亚稳相碳材料,如具有立方和六边形结构的纳米金刚石、面心立方金刚石、类 C_8 碳、碳洋葱、体心立方碳。同时,这一热力学非平衡态的激光液相烧蚀策略不仅局限于碳的亚稳相材料的设计,基于这一独特的晶体生长方式,研究人员合成了多种金属(双层六方铁、A15 相钨)[75-76]、半导体(面心立方硅、立方 GaN、四方结构 Ge)[77-79]、绝缘体(立方 ZrO_2、立方 BN、立方 C_3N_4)[80-82]等亚稳相材料。近年来,天津大学杜希文团队利用脉冲激光液相烧蚀技术首次合成了热力学平衡条件下难以互熔的钌金(RuAu)单原子合金,如图 5(g)~(i)所示,这一亚稳相材料单位活性位点的催化活性是商用 Pt/C 催化剂的 3 倍,表现出极高的稳定性和催化活性,为构建高性能的催化剂开辟了新思路。

综上所述,基于聚焦脉冲激光液相烧蚀策略,不仅可以实现多组分、多形貌纳米结构的可控调节,更重要的是,这一热力学非平衡态下的极端高温高压反应环境能够实现常规合成方法难以完成的亚稳相材料的构筑。

3　基于短波长激光液相辐照策略的贵金属复合构型的调控优化

基于激光与物质相互作用实现金属纳米复合材料的调控优化研究不仅体现在上述聚焦脉冲激光束的强烈烧蚀方式,还能表现为短波长激光束直接辐照(激光束的非聚焦情况)的温和模式。短波长激光辐照策略主要体现在两个方面:1)短波长激光束液相辐照具有带隙结构的半导体构型,基于激发产生的电子-空穴对,在半导体表面实现负载生长形成贵金属纳米复合构型;2)激光液相辐照贵金属纳米结构(Ag、Au 等),激发产生局域表面等离子体共振(LSPR),利用激发产生的热电子还原周围的金属离子,在纳米金属前驱体上进一步实现金属原子的沉积生长。

3.1　激光激发半导体材料优化设计贵金属复合构型

众所周知,具有典型带隙的半导体结构(TiO_2、

ZnO 等)在具有足够高能量($h\nu > E_g$,其中 h、ν、E_g 分别为普朗克常量、入射光子频率及半导体材料带隙)的光子辐照下,体系的电子通过吸收光子能量发生跃迁,从而产生电子-空穴对[23,83-84]。这种光激发的电子-空穴对在众多的光催化研究领域起到极为关键的作用,同时,这一独特过程还可以扩展到金属纳米材料负载生长,尤其是可将光生电子视为一种绿色高效的还原剂,实现周围液相中金属离子到金属原子的快速转变[24],进而在半导体表面成功负载生长贵金属纳米颗粒,最终构建表面洁净无污染的新型贵金属/半导体复合构型,这为后续的光激发以及光催化研究提供理想的纳米功能材料。

目前,基于短波长紫外(UV)光束的高光子能量与宽带隙半导体材料的相互作用已经可以原位地实现多种单金属(Au、Ag、Pt)、双金属(AuAg)纳米颗粒、金属氧化物等在半导体材料表面的可控负载生长,如图 6 所示。同时,研究人员也注意到激光诱导半导体产生的电子-空穴对极易复合,只有少量

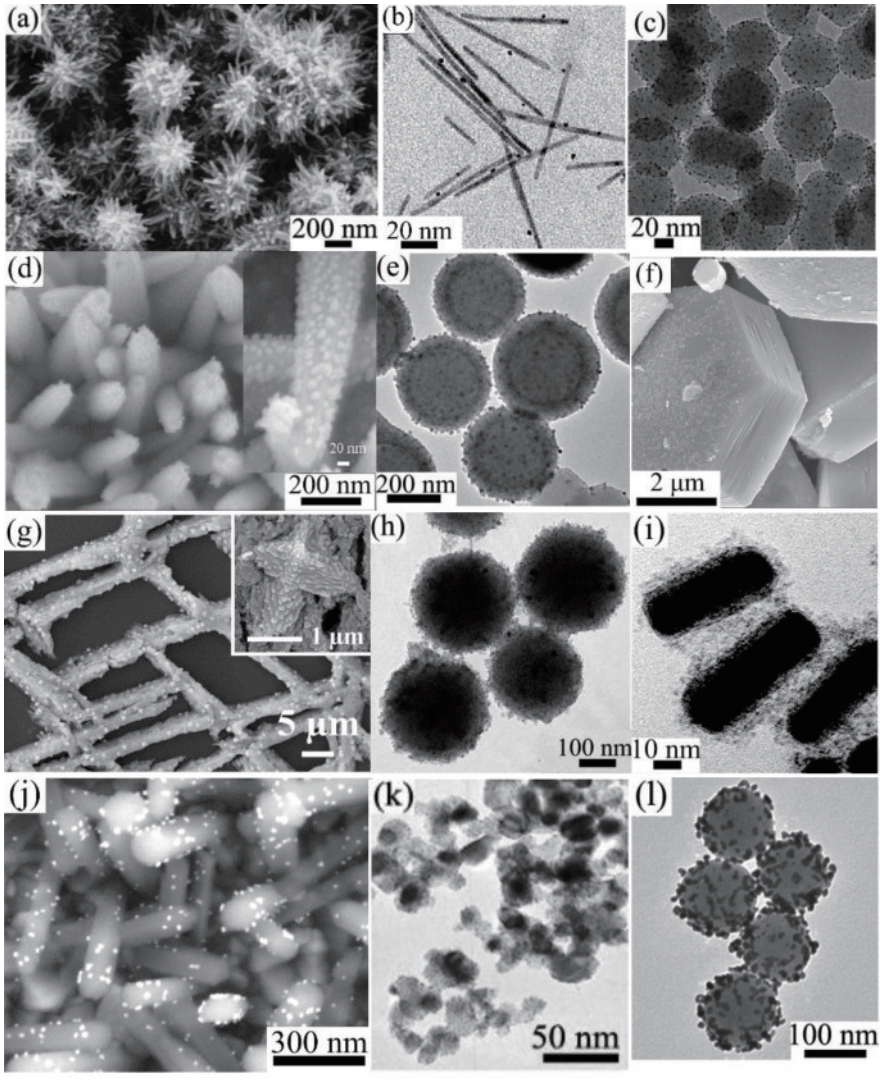

图 6　激光液相辐照激发电子-空穴对合成多种金属基复合结构[85-96]。(a)Mn_3O_4/H-TiO_2 复合物薄膜[85];(b)CdS/Pt 纳米棒[86];(c)SiO_2@Pt 纳米复合结构[87];(d)ZnO/Au 杂化纳米复合结构[88];(e)SiO_2@TiO_2-Ag[89];(f)Au 负载 ZnO 晶体[90];(g)Ag/ZnO[91];(h)Ag-SiO_2@α-Fe_2O_3 纳米复合球[92];(i)Au/AgNR/SnO_2[93];(j)ZnO/Au[94];(k)PtO_2/TiO_2 颗粒[95];(l)Au/Cdot-SiO_2纳米复合材料[96]

Fig. 6　Various composite nanostructures with metal substrates synthesized by electron-hole pairs generated by laser irradiation in liquid[85-96]. (a) Mn_3O_4/H-TiO_2 composite film[85]; (b) CdS/Pt nanorods[86]; (c) SiO_2@Pt nanocomposite structure[87]; (d) ZnO/Au hybrid nanocomposite structure[88]; (e) SiO_2@TiO_2-Ag[89]; (f) Au-loaded ZnO crystals[90]; (g) Ag/ZnO[91]; (h) Ag-SiO_2@α-Fe_2O_3 nanocomposites sphere[92]; (i) Au/AgNR/SnO_2[93]; (j) ZnO/Au[94]; (k) PtO_2/TiO_2 particles[95]; (l) Au/Cdot-SiO_2 nanocomposites[96]

的光生电子能够参与还原周围溶液中的金属离子，这极大地降低了负载生长金属纳米材料的产率，不利于贵金属的调控优化。为了有效地提高光生电子-空穴的分离效率，通常情况下，多种牺牲试剂被引入反应体系，用于消耗光生空穴，降低电子-空穴的复合率。在众多牺牲剂中，以乙醇为主的醇类小分子因其高度清洁的优势被广泛应用于光生空穴的俘获过程中，避免了后续纳米产物的清洗-除杂工艺。在一个典型的光诱导负载生长过程中，紫外激光作用于含有ZnO溶胶的$AgNO_3$溶液时，ZnO会吸收激光光子能量，使其表面产生电子，进而将溶液中的Ag离子还原为Ag原子，同时引入乙醇作为空穴的牺牲剂，其化学反应过程如下[91]：

$$ZnO + h\nu \rightarrow ZnO + e^- + h^+ \quad (\text{photoexcitation of ZnO}), \tag{1}$$

$$CH_3CH_2OH + 2h^+ \rightarrow CH_3CHO + 2H^+ \quad (\text{photooxidation}), \tag{2}$$

$$Ag^+ + e^- \rightarrow Ag^0 \quad (\text{photoreduction}), \tag{3}$$

式中：e^-和h^-分别代表电子和空穴。

后续研究还可以通过调节激光参数和液相环境参数得到不同负载情况的金属基复合材料构型，进而实现微观复合结构的优化设计[97-105]。

此外，依据上述的辐照机制，针对更为极端的宽带隙半导体结构，例如类石墨烯结构的氮化硼（>5 eV），显然必须提供波长更短的深紫外激光束，由此将明显提高调控制备的使用成本。另一方面，针对无带隙的石墨烯结构，通过上述的激光辐照思路同样难以在其表面负载生长贵金属纳米材料。鉴于此，研究人员选择对这些材料的表面进行有效的功能化修饰，通过酸碱处理、有机分子修饰等简单方式在其表面掺杂或附着大量的特定含氧官能团，如羟基、羧基等[106-121]。在此基础上再次通过紫外激光辐照技术对其表面的含氧官能团进行激发以产生活性电子，从而实现对溶液中金属离子的有效还原，可控地完成多种金属纳米颗粒的负载生长。基于这一反应机理，研究人员在功能化石墨烯、氮化硼、碳纳米管等多种类石墨烯结构上成功实现了不同金属纳米颗粒的负载生长[112-116]。

研究进一步表明，相比于单一组分纳米材料，采用激光液相辐照诱导这一新颖策略可以在半导体、功能化碳材料表面有效调控负载金属纳米颗粒构型，所形成的金属基复合纳米结构兼具原始基底材料与金属纳米颗粒各自独特的结构/性质优势，从而可以克服单一组分在实际应用中的局限性[85-89, 93, 110-116]。二者的有机结合不仅可以有效克服纯金属纳米颗粒易于团聚的弊端，同时能够实现对于基底能带结构的有效调控，最终使得金属基复合纳米结构的稳定性以及界面电子的传递能力均得到不同程度的提高。

3.2　基于激光辐照贵金属产生LSPR效应调控设计贵金属复合构型

众所周知，贵金属Ag、Au纳米材料经过外界光辐照激发，如果入射光场的频率与金属电子固有的振荡频率相匹配，纳米Ag、Au结构可以产生明显的LSPR效应，如图7(a)所示。基于贵金属Ag、Au特有的LSPR效应，当贵金属表面等离激元发生共振激发后，金属自由电子的集体振荡和迅速相移可以有效诱导产生热电子和热空穴的独特热载流子构型，如图7(b)所示。等离子诱导合成多种Ag纳米晶结构如图7(c)～(h)所示[118-123]。等离子驱动合成Au纳米片如图7(i)、(j)所示[124]。类似于光激发半导体结构，激光激发贵金属Ag、Au纳米材料诱导产生的热电子和热空穴也可以与周围溶液中的金属离子互相作用、参与化学反应，进而实现多种纳米结构的精细调节。自2001年Jin等[125]首次采用外界光诱导贵金属生长策略实现Ag纳米材料由零维球体调节为二维片状以来，引入激光束辐照方式作为Ag、Au微观结构的各向异性调控生长研究一直是科研人员的探索热点。前期研究工作主要基于激光诱导Ag纳米颗粒的LSPR效应，运用高活性Ag表面被激发的热电子还原周围溶液的Ag离子，实现了纳米片、纳米多面体、纳米立方体和纳米棒构型的精细调控生长，如图7(c)～(h)所示。由于Ag的化学活性较为活泼，在将各向同性的Ag前驱体向各向异性结构的调控过程中，如何全面阐述激光辐照诱导的热电子和热空穴在不同阶段所起到的作用及内在机制是长期面临的关键问题。直至2016年，Zhai等[126]率先将激光诱导贵金属结构调控扩展至可控合成化学性质稳定的Au纳米晶片，系统阐述了热载流子（热电子-空穴对）的界面传输方式在激光激发Au微观结构及后续异向生长中的作用模式。如图7(i)所示，基于532 nm激光辐照Au纳米前驱体，产生热电子和热空穴，利用聚乙烯吡咯烷酮（PVP）作为热电子还原周围溶液中Au离子的导向试剂，实现了Au原子沿着二维平面方向延展负载生长[图7(j)]。由于光激发Au产生的热电子和热空穴在几个飞秒内就会衰减回基态，研究人

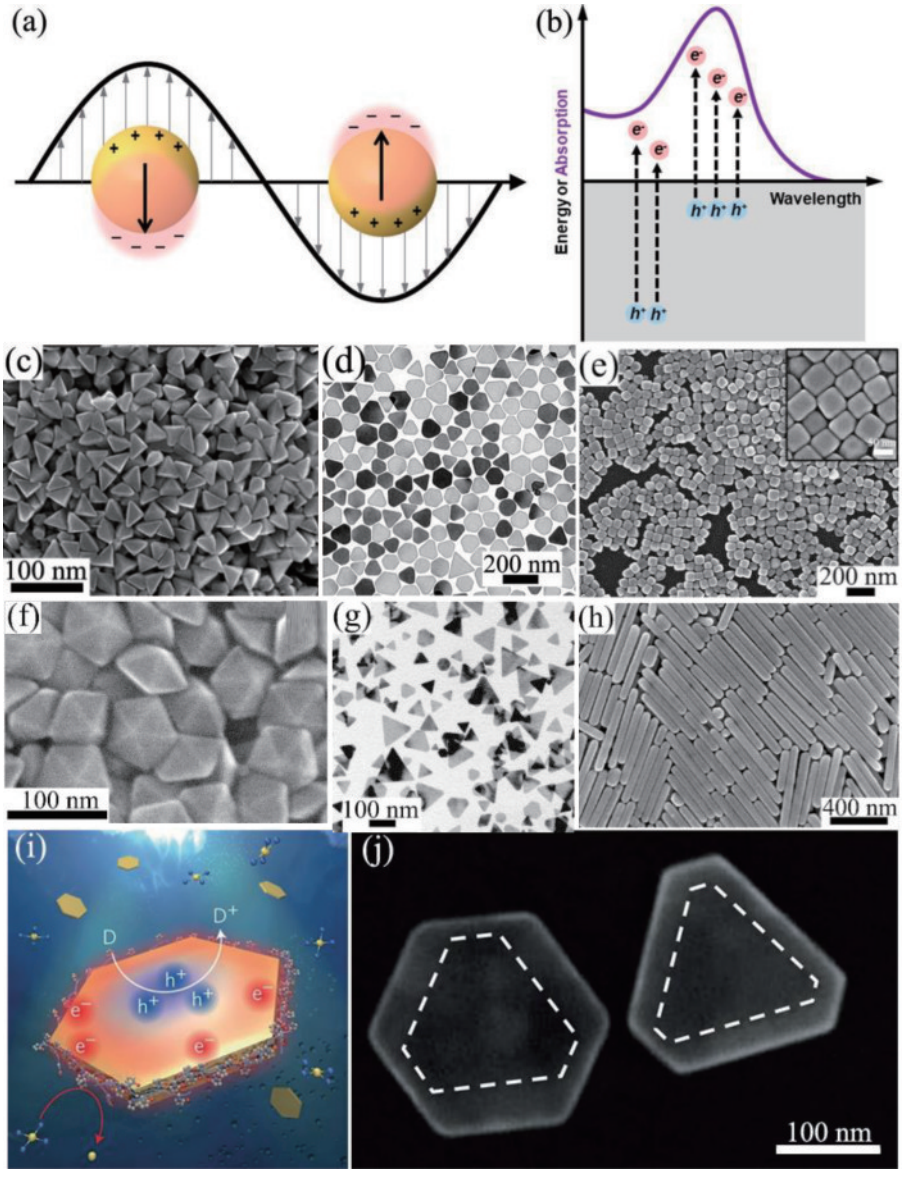

图7　基于激光辐照贵金属产生的LSPR效应合成金属基复合纳米结构。(a)电磁(EM)场引起的电子云的相干局域振荡[117]；(b)热载流子的产生和等离子体金属相应的吸收光谱[117]；(c)～(h)等离子体诱导合成多种Ag纳米晶结构[118-123]；等离子体驱动合成Au纳米片[124]：(i)Au纳米片的光化学生长示意图；(j)经光辐照形成的Au纳米片的扫描电子显微镜图像

Fig. 7　Nanocomposites with metal substrate synthesized by LSPR effect produced by laser irradiation of noble metals. (a) EM-field-induced coherent localized oscillation of electron cloud[117]; (b) hot carrier generation and corresponding absorption spectrum of plasmonic metals[117]; (c)–(h) plasmon-driven synthesis of various Ag nanostructures[118-123]; plasmon-driven synthesis of Au nanosheets[124]: (i) diagram of photochemical growth of Au nanosheet; (j) scanning electron microscopy image of Au nanosheet after irradiation

员在反应过程中创新性地引入绿色分子甲醇作为热空穴的捕获试剂，提高了溶液中Au^{3+}离子的还原效率。受此启发，Xu等[127]将乙醇作为热空穴的牺牲试剂，采用532 nm连续激光辐照技术成功地在Au纳米枝的表面负载生长了均匀的Ag原子，利用激光诱导的光化学方法制备了小尺寸的组分可调的AuAg双金属纳米枝。目前，基于激光液相辐照贵金属Ag、Au纳米前驱体产生的LSPR效应，扩展研究已经被广泛应用于多种新型金属复合材料的合成，如Au-Ag复合二十面体、AgFON/Cu NP薄膜、Pt-Au纳米棒、Ag-Pt复合纳米材料等[128-131]。由此可见，基于激光诱导贵金属Ag、Au纳米结构的LSPR效应所产生的热载流子能够应用到微观结构各向异性生长的有效调控研究，这为后续更为复杂

的多功能复合构型的优化设计提供了一种新颖的可行性方案。此外，通过有效调节激光参数可以精确地调控各金属组分之间的配比，实现最佳的电子耦合和协同效果。相比于单金属纳米材料，基于激光液相辐照贵金属结构所激发的LSPR效应优化设计出的多元金属组分的复合结构可以充分彰显出多金属之间的协同效应[127-131]，由此获得更为优异的光学、电学、热学和催化性能，这些性能在更为广泛的实际应用中具有显著优势。

综上所述，采用具有高能量光子的短波长激光束液相辐照诱导调控策略可以直接激发具有能带结构的基底材料（包括半导体、功能化碳材料）以及具有LSPR效应的贵金属构型，产生的大量光生电子能够作为高效的绿色还原剂，最终在前驱体材料上实现金属纳米颗粒的有效负载生长，由此构建出多功能化的金属基复合纳米材料。基于短波长激光液相辐照调控优化策略，可以最大限度地降低常规化学合成在负载生长贵金属过程中对前驱体结构的损坏，这有利于所合成的复合构型充分集成前驱体的优异物理/化学性能。

4　光激发应用研究进展

基于激光液相调控优化设计的金属基纳米复合构型作为一种新兴材料，其表面洁净的可调谐金属原子展现出了显著增强的受光照激发特性，被广泛应用于表面增强拉曼散射、光催化、近红外强吸收等领域。在此，结合已有的研究工作对其具体应用展开描述。

4.1　表面增强拉曼散射（SERS）应用

表面增强拉曼散射（SERS）因其超高灵敏性和无损检测的特点已经发展成为一种强有力的光谱分析技术，广泛应用于生物医学、食品安全、环境科学、催化、微量元素分析等领域[132-140]，如图8所示。众所周知，SERS现象是指当一些分子或离子（如吡

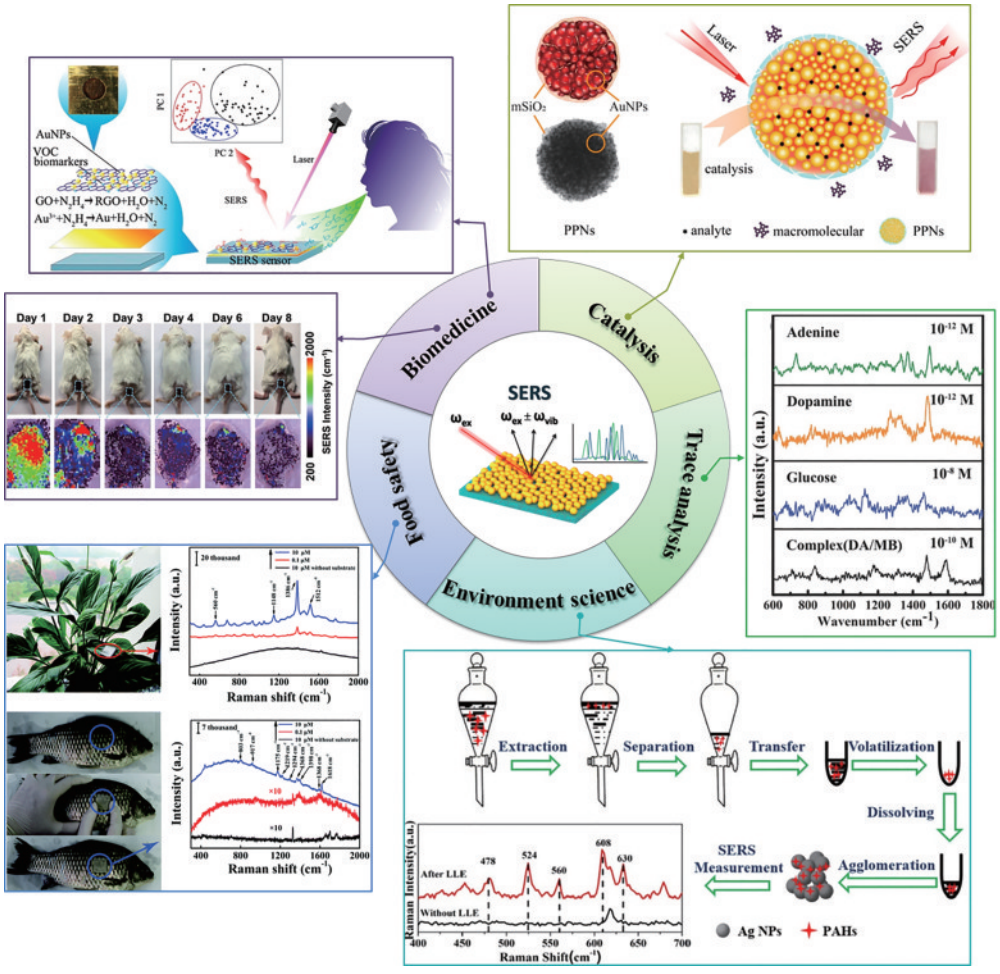

图8　SERS在实际领域如生物医学、食品安全、环境科学、催化以及痕量分析中的应用[132-138]

Fig. 8　Extensive applications of SERS, including biomedicine, food safety, environmental science, catalysis, and trace analysis[132-138]

啶、氰离子)吸附在Ag、Au等贵金属纳米材料表面后,这些分子或离子的拉曼散射光谱的强度得以显著提高10^5~10^{14}倍,这有利于低浓度的分子探测,尤其是经过近40年的不断努力,SERS研究已经达到了单分子的超灵敏检测水平[141-146],为深入探索生物医学领域微量细胞分子在新陈代谢中的结构转化提供了新的机遇。根据经典理论,被测分子拉曼光谱的强度与感应偶极矩的平方成正比,这是分子极化率与所施加电场的乘积[147-150]。相比于分子极化引起的化学增强因素,分子周围电磁场强度的提高所导致的物理增强机制在提高SERS性能过程中占据主导地位。贵金属Ag、Au纳米材料因其固有的LSPR效应,在外界光的激发下可以在其表面形成局域增强的电磁场,以有效调控优化Ag、Au的微观界面构型(例如复合结构的金属组分、整体形貌、界面原子洁净度以及空间排布等),极大地提高电磁场强度,这是优化SERS基底并高效提高SERS活性的至关重要环节[151-166]。研究贵金属纳米材料的组分和结构是优化其在实际应用中高性能的先决条件,基于此,采用激光调控优化设计的多种优异超纯构型的贵金属复合材料在SERS应用研究领域具有显著的优势。

在构建高活性的SERS纳米基底研究中,调控制备多枝状AgAu双金属微观构型既可以充分利用众多的纳米针尖结构能够被光激发产生显著增强的电磁场进而极大地提高SERS物理增强效果的特点,又可以发挥双金属之间的协同效应用以有效提高双金属受光激发的自由电子集体振荡的程度,进而加剧光子与金属电子之间相互作用的效果[151-155]。这一独特的AgAu构型在SERS应用研究中备受关注,然而,构建这种多枝状结构通常需要借助于十六烷基三甲基溴化铵(CTAB)或PVP作为辅助定向生长试剂,后续产物的除杂工艺极为苛刻,而且在确保多枝状纳米构型的基础上如何有效调控双金属的组分进而实现SERS活性的最优化一直是常规可控合成的巨大挑战。2017年,Xu等[127]采用532 nm连续激光诱导的光化学反应在对已有Au纳米枝结构无损伤的前提下实现了负载Ag的可控生长,完成了对于Ag@Au纳米枝中Ag的质量分数在1.2%~34%范围内的可控调节。此外,激光诱导合成过程中避免使用辅助试剂,确保了合成产物表面原子的洁净无污染。最后,将组分可调的Ag@Au纳米枝作为SERS基底检测分析了极低含量的水溶性有毒硫化物质:4-氨基苯硫酚(4-ATP)分子,研究表明:利用表面洁净无污染的多枝状Ag@Au纳米材料可以达到的SERS探测极限低至~10^{-14} mol/L,计算得到的增强因子为~10^{11}。由此获得的超低浓度分子SERS探测将促进多枝状Ag@Au纳米结构成为一种具有显著竞争优势的SERS基底,同时也证实了激光诱导光化学方法可作为一种合成多组分贵金属纳米材料的通用有效策略。

考虑到单纯贵金属纳米材料基底由于使用成本高、稳定性较低、重复性差等缺陷严重阻碍了其在SERS实际环境中的应用,已有SERS研究开始致力于廉价半导体材料基底的开发,尤其是宽带隙半导体(ZnO、TiO_2等)[167-170]。与贵金属材料相比,半导体材料具有出色的可回收性、较长的使用寿命和高成本效益等优势。然而,单纯的半导体材料SERS基底增强主要基于材料与探针分子之间的电荷转移机制,难以直接用于实现探测分子的超灵敏检测。如果将少量贵金属纳米颗粒负载生长到半导体结构表面,将会充分发挥两者各自的优势。利用半导体的光生载流子效应,Xu等[97-98]将紫外激光束诱导的光化学反应扩展至半导体表面负载超纯的金属纳米颗粒,成功制备了ZnO@Au纳米棒以及ZnO@Ag纳米片复合材料基底。综合贵金属受激发产生电磁场的物理增强机制和半导体与探针分子之间的电荷转移引起的化学增强机制,利用最终优化设计的金属/半导体复合材料实现了废水中有机染料分子结晶紫(CV)、甲基蓝(MB)的超灵敏检测。其中,基于ZnO@Au纳米棒增强的光催化降解特性,利用紫外光照射含有MB分子的SERS基底30 min后可以将有机污染物几乎完全去除。经过20次循环测试,所得基底依旧表现出优异的SERS活性。由此可见,激光诱导光化学法合成的新型ZnO@Au纳米棒复合材料可以作为一种高稳定性和可循环使用的SERS基底,用于废水中耐光染料分子的超灵敏检测,以达到早期发现早期治理的目的。

此外,功能化二维(2D)材料负载生长贵金属(Au,Ag)纳米颗粒作为一种新型复合材料基底在SERS研究中逐渐呈现出明显优势。与传统胶体金属相比,此类复合材料有望作为高活性、高稳定性的SERS基底主要得益于以下三个方面:1)2D材料基底可以有效避免负载贵金属纳米颗粒的团聚现象,进而提高SERS基底的活性和稳定性[171-173];

2)2D材料固有的较大比表面积以及面内碳原子之间的sp^2杂化能够通过π-π堆积或静电相互作用极大地提高含有苯环的芳香族探针分子的吸附能力[174-176],进而实现SERS的超低浓度检测;3)除了源于贵金属纳米颗粒的LSPR效应产生的电磁场(EM)增强以外,2D材料载体与探针分子之间有效的电荷传输可以提供额外的化学增强(CM),这进一步增强了SERS活性[177-178]。Chen课题组采用紫外波长的连续激光束液相辐照策略实现了氧化石墨烯(GO)、六方氮化硼(h-BN)以及羟基化碳纳米管(CNTs)负载生长金属纳米颗粒,成功制备了高活性、高稳定性的GO/Au NPs、h-BN/Au、h-BN/CuAg、CNT/Au@Ag NPs复合材料SERS基底[115-116, 179-180]。利用上述表面洁净的SERS基底不仅实现了多种有机染料分子如结晶紫、罗丹明6G、孔雀石绿、亚甲基蓝等痕量检测以及多种有机染料分子的同时分辨,也实现了生物分子肌酸酐、番茄表皮残留农药三环唑分子的超低浓度探测。

4.2　光催化

光催化作为一种新型科学,在环境净化、光解水制氢、太阳能光伏电池以及CO_2能源转化等方面具有非常诱人的应用前景,受到环境、材料、化学和能源领域研究人员的广泛关注[181-187]。作为一种可持续发展的方法,光催化在实现太阳能向化学能的有效转化方面具有巨大应用潜力,被认为是直接获取、转换和储存太阳能以产生可持续能源最具吸引力和前景的技术之一。近年来,光催化研究主要关注于半导体结构受光照激发产生的导带上还原性的电子与价带上氧化性的空穴,以诱发后续的氧化还原反应。而且以Au、Ag、Cu等金属纳米结构的可见光吸收为驱动力的光催化能够解决宽带隙半导体(半导体材料带隙E_g>3.0 eV)局限在紫外光催化研究的瓶颈[188-192]。基于此,通过激光液相诱导策略优化设计的多种金属基复合材料有望作为新型光催化剂广泛应用于光催化的众多研究领域中。

半导体纳米材料(TiO_2、ZnO、CdS、WO_3等)具有极高的化学稳定性、优异的光电性能、成本低廉、环境友好等诸多优点,被认为是最具应用前景的光催化剂之一[193-197]。然而,在实际应用场景中,该类光催化剂固有的宽带隙特点使其对于太阳光的吸收仅局限在紫外区域,这大大降低了对于太阳光的利用率[23-24,84]。为了提高半导体材料对于太阳能的吸收和转化,通过半导体掺杂、金属掺杂、构建复合结构等途径拓宽其吸收波长范围是当前半导体光催化研究中的重点。目前,科研人员通过利用激光液相辐照策略诱导半导体沉积贵金属这一温和手段构建金属/半导体复合构型的方式极大地改善了半导体材料的光催化性能。以宽带隙半导体TiO_2为例,基于短波紫外光液相辐照的方式,研究人员已经成功在其表面分别负载生长了多种贵金属Au、Ag、Cu、Pt等,该方式有效地提高电子、空穴的分离能力,增强了催化剂对于可见光的收集能力,进而开发了多种高性能的金属/半导体复合的光催化剂,上述方式对于其他宽带隙半导体同样具有普适性[99-105]。

研究表明,基于高能脉冲激光液相烧蚀策略构筑的多种金属基纳米材料同样具备高效的光催化活性以及独特的表面反应活性[60, 65, 198-208],这使其在光催化领域发挥着重要的应用价值。Zeng等[198]使用1064 nm高能脉冲激光烧蚀十二烷基硫酸钠水溶液中的固体锌片,成功合成了具有超高活性的Zn/ZnO核壳纳米结构,以此为模板并通过进一步弱酸选择性刻蚀成功设计出具有优异光催化活性、高稳定性的ZnO、Au/ZnO、Pt/ZnO和Au/Pt/ZnO空心纳米颗粒并实现了对于有机染料甲基橙的高效降解。同时,该课题组通过进一步深入研究指出Pt/ZnO多孔纳米笼状结构要比同一组分的笼状结构表现出更为优异的光催化活性,其主要原因可以归结为多孔笼状结构具有更大的比表面积以及更强的电子-空穴分离能力[199]。此外,Chen课题组通过脉冲激光简单烧蚀活性液体中的固体Sn靶,成功制备了超小尺寸(<10 nm)的高纯度、高稳定性多孔Sn_2S_3纳米颗粒光催化剂,实现了可见光下六价态重金属镉离子的快速降解[200]。除了上述简单的金属氧化物外,研究人员利用激光液相烧蚀技术开发了多种复杂的纳米结构以改善光催化降解性能,例如核壳结构、层次球、立方体和海胆状三元氧化物以及三维有序结构等[60, 65, 201-202]。Li等[201]巧妙构建了具有核壳结构的新型$Ta_xO@Ta_2O_5$纳米颗粒,其中低氧的Ta_xO核因其增强的光吸收及高效的捕获电子能力被认为是提升光活性的至关重要部分。为了实现光催化反应中催化剂的循环利用,Liang等[60]成功制备了栗子状的$Fe_3O_4@C@ZnSnO_3$核-壳颗粒,基于独特碳层的保护作用,该核壳结构光催化剂展现出了优异的循环特性。此外,Cai等[203]通过水热处理和激光液相烧蚀相结合的方式巧妙地

在管状 TiO_2 阵列上复合层状 $ZnTiO_3$ 纳米片，形成了简单的 $TiO_2/ZnTiO_3$ 异质结，这一新型异质结构的独特之处在于具有有利于电子传输的低电阻界面层。基于相同的合成手段，立方状 Zn_2SnO_4 和类海胆的 $ZnSnO_3$ 纳米材料已被用于有效地去除废水中的有机染料甲基橙和 2，5-二氯苯酚[65]。尽管上述基于激光液相烧蚀策略构筑的多种金属基纳米结构表现出了较高的光催化性能，但是其对于太阳光的利用率依旧相对较低，仅停留在紫外波段。为了解决上述问题，研究人员基于该策略合成了多种具有可见光响应的光催化剂[204-208]。研究发现，TiO_2 和 α-Fe_2O_3 核壳纳米颗粒的能级可以相互匹配以达到增强可见光催化的目的[204]，基于此，科研人员采用激光方法将二者完美结合。α-Fe_2O_3 是 n 型半导体，具有 2.2 eV 的窄带隙，它对于太阳光的收集能力是带隙为 3.2 eV 的 TiO_2 太阳能收集器的 15 倍。同时，该复合结构的良好匹配界面及其对于氧气的吸附作用，使其对应的光生电子-空穴对分离能力得到了显著提高。此外，Lin 等[205]采用激光液相烧蚀策略首次一步合成了具有高效可见光催化活性的超纯 Ag/AgCl 等离子体立方体催化剂。该结构中 Ag 纳米颗粒固有的 LSPR 效应极大地增强了其对于可见光的利用率，最终实现了对于多种有机染料 MO、RhB 和 MB 的高效可循环的可见光催化降解，这为激光液相烧蚀策略应用于其他金属/卤化物新型光催化剂的构建提供了依据。除此之外，科研人员基于激光液相诱导策略制备的多种超纯高活性的光催化剂，如 CdS-PdPt 纳米复合材料、CoO 纳米晶、ND-Cu_2O 纳米晶等，也被广泛应用于光解水制氢、太阳能电池等领域[209-212]。

综上所述，基于激光液相辐照策略合成的具有清洁表面和丰富缺陷的金属复合纳米材料因其优异的光激发特性，有望发展成为新型的高性能光催化剂。

4.3　其他应用

除了上述涉及领域外，基于激光液相调控策略构筑的多种金属基复合材料如 Au/TiO_2 纳米枝、多枝状 CuS 纳米晶、GNR/rGO 复合材料等均表现出较强的近红外吸收特性，有望作为光热治疗手段的优选光热试剂[213-215]。此外，杨国伟课题组基于激光液相烧蚀策略合成了一种全新的高性能光热转换全介质材料，即碲(Te)纳米颗粒[216]。研究表明，该材料自组装形成的吸收层表现出强烈的宽谱吸收属性，在整个太阳光谱范围内的吸收率超过 85%(紫外区接近 100%)。此外，仅通过 100 s 的太阳光照射，该吸收层的温度便可以从 29 ℃上升至 85 ℃。由此可见，基于激光液相烧蚀策略制备的碲纳米颗粒不仅可以实现全太阳光谱吸收，而且具有极高的光热转换效率，在太阳能光热转换海水淡化领域发挥着重要作用。由此可见，激光液相诱导优化设计金属基纳米材料这一独特策略为功能化纳米材料的多领域应用提供了无限可能。

5　结　　论

激光液相加工调控技术已经发展成为一种优化金属基复合构型的有效途径。基于非平衡状态下极短瞬间的高能脉冲激光聚焦烧蚀和平衡状态下短波段高光子连续激光辐照两种方式借助简单的液相环境构筑的金属复合材料具有表面纯净、稳定性高、成本低等多种优势，可用于以 SERS 最为典型的光激发领域。总结了激光液相诱导技术的方式和原理，并着重探讨了其优化设计的金属复合构型在 SERS、光催化、近红外强吸收等领域的应用潜力，该策略有望发展成为金属基复合材料调控设计方面更为经济的普适手段。

参　考　文　献

[1] Park M, Jung H, Jeong Y, et al. Plasmonic schirmer strip for human tear-based gouty arthritis diagnosis using surface-enhanced Raman scattering [J]. ACS Nano, 2017, 11(1): 438-443.

[2] Zhang S D, Geryak R, Geldmeier J, et al. Synthesis, assembly, and applications of hybrid nanostructures for biosensing [J]. Chemical Reviews, 2017, 117(20): 12942-13038.

[3] Lin Z S, He L L. Recent advance in SERS techniques for food safety and quality analysis: a brief review [J]. Current Opinion in Food Science, 2019, 28: 82-87.

[4] Cai B, Henning S, Herranz J, et al. Nanostructuring noble metals as unsupported electrocatalysts for polymer electrolyte fuel cells [J]. Advanced Energy Materials, 2017, 7(23): 1700548.

[5] Liu X Q, Iocozzia J, Wang Y, et al. Noble metal-metal oxide nanohybrids with tailored nanostructures for efficient solar energy conversion, photocatalysis and environmental remediation [J]. Energy & Environmental Science, 2017, 10(2): 402-434.

[6] Loza K, Heggen M, Epple M. Synthesis, structure,

properties, and applications of bimetallic nanoparticles of noble metals[J]. Advanced Functional Materials, 2020, 30(21): 1909260.

[7] Gilroy K D, Ruditskiy A, Peng H C, et al. Bimetallic nanocrystals: syntheses, properties, and applications[J]. Chemical Reviews, 2016, 116(18): 10414-10472.

[8] Mangadlao J D, Cao P F, Choi D, et al. Photoreduction of graphene oxide and photochemical synthesis of graphene-metal nanoparticle hybrids by ketyl radicals[J]. ACS Applied Materials & Interfaces, 2017, 9(29): 24887-24898.

[9] Chen Z, Liu C, Cao F, et al. DNA metallization: Principles, methods, structures, and applications[J]. Chemical Society Reviews, 2018, 47(11): 4017-4072.

[10] Koczkur K M, Mourdikoudis S, Polavarapu L, et al. Polyvinylpyrrolidone (PVP) in nanoparticle synthesis [J]. Dalton Transactions (Cambridge, England, 2015, 44(41): 17883-17905.

[11] Dong H, Zhang C, Liu X, et al. Materials chemistry and engineering in metal halide perovskite lasers [J]. Chemical Society Reviews, 2020, 49(3): 951-982.

[12] Zhang D S, Gökce B, Barcikowski S. Laser synthesis and processing of colloids: Fundamentals and applications [J]. Chemical Reviews, 2017, 117(5): 3990-4103.

[13] Wang X S, Huang Y K, Shen B, et al. Advances of short and ultrashort pulse laser induced plasma micromachining [J]. Laser & Optoelectronics Progress, 2020, 57(11): 111405.
王兴盛, 黄宇珂, 沈博, 等. 短/超短脉冲激光诱导等离子体微加工研究进展[J]. 激光与光电子学进展, 2020, 57(11): 111405.

[14] Palneedi H, Park J H, Maurya D, et al. Laser processing of metal oxides: Laser irradiation of metal oxide films and nanostructures: applications and advances (adv. mater. 14/2018)[J]. Advanced Materials, 2018, 30(14): 1870094.

[15] Gökce B, Filipescu M, Barcikowski S. Recent progress in laser materials processing and synthesis [J]. Applied Surface Science, 2020, 513: 145762.

[16] Fan L S, Zhang S W, Zhang Q L, et al. Research progress on fabrication of one-dimensional well-ordered oxide nanostructures by pulsed laser deposition [J]. Laser & Optoelectronics Progress, 2020, 57(19): 190001.
范丽莎, 张硕文, 张群莉, 等. 脉冲激光沉积制备一维有序氧化物纳米结构的研究进展[J]. 激光与光电子学进展, 2020, 57(19): 190001.

[17] Pan B, Xiao J, Li J, et al. Carbyne with finite length: The one-dimensional sp carbon[J]. Science Advances, 2015, 1(9): e1500857.

[18] Chen C H, Wu D Y, Li Z, et al. Ruthenium-based single-atom alloy with high electrocatalytic activity for hydrogen evolution [J]. Advanced Energy Materials, 2019, 9(20): 1803913.

[19] Li Z, Fu J Y, Feng Y, et al. A silver catalyst activated by stacking faults for the hydrogen evolution reaction [J]. Nature Catalysis, 2019, 2(12): 1107-1114.

[20] Kabashin A V, Singh A, Swihart M T, et al. Laser-processed nanosilicon: A multifunctional nanomaterial for energy and healthcare[J]. ACS Nano, 2019, 13(9): 9841-9867.

[21] Liu H, Jin P, Xue Y M, et al. Photochemical synthesis of ultrafine cubic boron nitride nanoparticles under ambient conditions [J]. Angewandte Chemie International Edition, 2015, 54(24): 7051-7054.

[22] Ravnik J, Vaskivskyi I, Gerasimenko Y, et al. Strain-induced metastable topological networks in laser-fabricated TaS_2 polytype heterostructures for nanoscale devices[J]. ACS Applied Nano Materials, 2019, 2(6): 3743-3751.

[23] Weng B, Qi M Y, Han C, et al. Photocorrosion inhibition of semiconductor-based photocatalysts: Basic principle, current development, and future perspective[J]. ACS Catalysis, 2019, 9(5): 4642-4687.

[24] Wenderich K, MethodsMul G. Mechanism, and applications of photodeposition in photocatalysis: A review [J]. Chemical Reviews, 2016, 116(23): 14587-14619.

[25] Wang N N, Guan B, Zhao Y, et al. Sub-10 nm Ag nanoparticles/graphene oxide: Controllable synthesis, size-dependent and extremely ultrahigh catalytic activity[J]. Small, 2019, 15(23): 1901701.

[26] Pérez-Mayoral E, Calvino-Casilda V, Soriano E. Metal-supported carbon-based materials: Opportunities and challenges in the synthesis of valuable products[J]. Catalysis Science & Technology, 2016, 6(5): 1265-1291.

[27] Sutter P, Li Y, Argyropoulos C, et al. *In situ* electron microscopy of plasmon-mediated nanocrystal synthesis [J]. Journal of the American Chemical Society, 2017,

139(19): 6771-6776.

[28] Amendola V, Meneghetti M. Laser ablation synthesis in solution and size manipulation of noble metal nanoparticles[J]. Physical Chemistry Chemical Physics, 2009, 11(20): 3805-3821.

[29] Yang G W. Laser ablation in liquids: Applications in the synthesis of nanocrystals[J]. Progress in Materials Science, 2007, 52(4): 648-698.

[30] Amendola V, Meneghetti M. What controls the composition and the structure of nanomaterials generated by laser ablation in liquid solution? [J]. Physical Chemistry Chemical Physics, 2013, 15(9): 3027-3046.

[31] Xiao J, Liu P, Wang C X, et al. External field-assisted laser ablation in liquid: An efficient strategy for nanocrystal synthesis and nanostructure assembly [J]. Progress in Materials Science, 2017, 87: 140-220.

[32] Saraeva I N, Kudryashov S I, Rudenko A A, et al. Effect of fs/ps laser pulsewidth on ablation of metals and silicon in air and liquids, and on their nanoparticle yields[J]. Applied Surface Science, 2019, 470: 1018-1034.

[33] Lam J, Amans D, Chaput F, et al. Γ-Al_2O_3 nanoparticles synthesised by pulsed laser ablation in liquids: A plasma analysis [J]. Physical Chemistry Chemical Physics: PCCP, 2014, 16(3): 963-973.

[34] Dell'Aglio M, Gaudiuso R, De Pascale O, et al. Mechanisms and processes of pulsed laser ablation in liquids during nanoparticle production [J]. Applied Surface Science, 2015, 348: 4-9.

[35] Perez D, Béland L K, Deryng D, et al. Numerical study of the thermal ablation of wet solids by ultrashort laser pulses[J]. Physical Review B, 2008, 77: 014108.

[36] Tan D Z, Zhou S F, Qiu J R, et al. Preparation of functional nanomaterials with femtosecond laser ablation in solution [J]. Journal of Photochemistry and Photobiology C: Photochemistry Reviews, 2013, 17: 50-68.

[37] Sakka T, Masai S, Fukami K, et al. Spectral profile of atomic emission lines and effects of pulse duration on laser ablation in liquid [J]. Spectrochimica Acta Part B: Atomic Spectroscopy, 2009, 64(10): 981-985.

[38] de Giacomo A, Dell'Aglio M, Santagata A, et al. Cavitation dynamics of laser ablation of bulk and wire-shaped metals in water during nanoparticles production[J]. Physical Chemistry Chemical Physics: PCCP, 2013, 15(9): 3083-3092.

[39] Liu K, Chen J, Qu H S, et al. Bubble dimer dynamics induced by dual laser beam ablation in liquid[J]. Applied Physics Letters, 2018, 113(2): 021902.

[40] Yang C, Feng G Y, Dai S Y, et al. Femtosecond pulsed laser ablation in microfluidics for synthesis of photoluminescent ZnSe quantum dots [J]. Applied Surface Science, 2017, 414: 205-211.

[41] Arce V B, Santillán J M J, Muñetón Arboleda D, et al. Characterization and stability of silver nanoparticles in starch solution obtained by femtosecond laser ablation and salt reduction [J]. The Journal of Physical Chemistry C, 2017, 121(19): 10501-10513.

[42] Labutin T A, Lednev V N, Ilyin A A, et al. Femtosecond laser-induced breakdown spectroscopy [J]. Journal of Analytical Atomic Spectrometry, 2016, 31(1): 90-118.

[43] Wang J B, Yang G W. Phase transformation between diamond and graphite in preparation of diamonds by pulsed-laser induced liquid-solid interface reaction[J]. Journal of Physics: Condensed Matter, 1999, 11(37): 7089-7094.

[44] Yang L, May P W, Yin L, et al. Growth of diamond nanocrystals by pulsed laser ablation of graphite in liquid [J]. Diamond and Related Materials, 2007, 16(4/5/6/7): 725-729.

[45] Du X W, Qin W J, Lu Y W, et al. Face-centered-cubic Si nanocrystals prepared by microsecond pulsed laser ablation[J]. Journal of Applied Physics, 2007, 102(1): 013518.

[46] Wei S Y, Yamamura T, Kajiya D, et al. White-light-emitting silicon nanocrystal generated by pulsed laser ablation in supercritical fluid: investigation of spectral components as a function of excitation wavelengths and aging time [J]. The Journal of Physical Chemistry C, 2012, 116(6): 3928-3934.

[47] Liang Y, Liu P, Li H B, et al. Synthesis and characterization of copper vanadate nanostructures via electrochemistry assisted laser ablation in liquid and the optical multi-absorptions performance [J]. CrystEngComm, 2012, 14(9): 3291-3296.

[48] Yang S K, Kiraly B, Wang W Y, et al. Fabrication and characterization of beaded SiC quantum rings with anomalous red spectral shift[J]. Advanced Materials, 2012, 24(41): 5598-5603.

[49] Yang L, May P W, Yin L, et al. Ultra fine carbon

nitride nanocrystals synthesized by laser ablation in liquid solution[J]. Journal of Nanoparticle Research, 2007, 9(6): 1181-1185.

[50] Xiao J, Wu Q L, Liu P, et al. Highly stable sub-5 nm $Sn_6O_4(OH)_4$ nanocrystals with ultrahigh activity as advanced photocatalytic materials for photodegradation of methyl orange [J]. Nanotechnology, 2014, 25(13): 135702.

[51] Zhang H W, Duan G T, Li Y, et al. Leaf-like tungsten oxide nanoplatelets induced by laser ablation in liquid and subsequent aging[J]. Crystal Growth & Design, 2012, 12(5): 2646-2652.

[52] Zhang H M, Liang C H, Tian Z F, et al. Organization of Mn_3O_4 nanoparticles into γ-MnOOH nanowires via hydrothermal treatment of the colloids induced by laser ablation in water[J]. CrystEngComm, 2011, 13(4): 1063-1066.

[53] Niu K Y, Yang J, Kulinich S A, et al. Morphology control of nanostructures via surface reaction of metal nanodroplets [J]. Journal of the American Chemical Society, 2010, 132(28): 9814-9819.

[54] Genc Oztoprak B, Akman E, Hanon M M, et al. Laser welding of copper with stellite 6 powder and investigation using LIBS technique [J]. Optics & Laser Technology, 2013, 45: 748-755.

[55] Yan Z J, Bao R Q, Chrisey D B. Self-assembly of zinc hydroxide/dodecyl sulfate nanolayers into complex three-dimensional nanostructures by laser ablation in liquid [J]. Chemical Physics Letters, 2010, 497(4/5/6): 205-207.

[56] Fu H, Liu G Q, Bao H M, et al. Ultrathin hexagonal PbO nanosheets induced by laser ablation in water for chemically trapping surface-enhanced Raman spectroscopy chips and detection of trace gaseous H_2S[J]. ACS Applied Materials & Interfaces, 2020, 12(20): 23330-23339.

[57] Liang Y, Liu P, Xiao J, et al. A microfibre assembly of an iron-carbon composite with giant magnetisation [J]. Scientific Reports, 2013, 3: 3051.

[58] Luo R C, Li C, Du X W, et al. Direct conversion of bulk metals to size-tailored, monodisperse spherical non-coinage-metal nanocrystals [J]. Angewandte Chemie International Edition, 2015, 54(16): 4787-4791.

[59] Xiao J, Liu P, Liang Y, et al. High aspect ratio β-MnO_2 nanowires and sensor performance for explosive gases[J]. Journal of Applied Physics, 2013, 114(7): 073513.

[60] Liang D W, Wu S L, Wang P P, et al. Recyclable chestnut-like Fe_3O_4@C@$ZnSnO_3$ core-shell particles for the photocatalytic degradation of 2,5-dichlorophenol [J]. RSC Advances, 2014, 4(50): 26201-26206.

[61] Liu P, Liang Y, Lin X Z, et al. A general strategy to fabricate simple polyoxometalate nanostructures: Electrochemistry-assisted laser ablation in liquid[J]. ACS Nano, 2011, 5(6): 4748-4755.

[62] Liu J, Cai Y Y, Tian Z F, et al. Highly oriented Ge-doped hematite nanosheet arrays for photoelectrochemical water oxidation[J]. Nano Energy, 2014, 9: 282-290.

[63] Liang Y, Liu P, Li H B, et al. $ZnMoO_4$ micro- and nanostructures synthesized by electrochemistry-assisted laser ablation in liquids and their optical properties[J]. Crystal Growth & Design, 2012, 12(9): 4487-4493.

[64] Yan Z J, Compagnini G, Chrisey D B. Generation of AgCl cubes by excimer laser ablation of bulk Ag in aqueous NaCl solutions [J]. The Journal of Physical Chemistry C, 2011, 115(12): 5058-5062.

[65] Tian Z F, Liang C H, Liu J, et al. Zinc stannate nanocubes and nanourchins with high photocatalytic activity for methyl orange and 2, 5-DCP degradation [J]. Journal of Materials Chemistry, 2012, 22(33): 17210-17214.

[66] Ran P, Jiang L, Li X, et al. Femtosecond photon-mediated plasma enhances photosynthesis of plasmonic nanostructures and their SERS applications[J]. Small, 2019, 15(11): 1804899.

[67] Shao Q, Wang Y, Yang S Z, et al. Stabilizing and activating metastable nickel nanocrystals for highly efficient hydrogen evolution electrocatalysis[J]. ACS Nano, 2018, 12(11): 11625-11631.

[68] Barth S, Seifner M S, Maldonado S. Metastable group IV allotropes and solid solutions: Nanoparticles and nanowires[J]. Chemistry of Materials, 2020, 32(7): 2703-2741.

[69] Fu Y P, Wu T, Wang J, et al. Stabilization of the metastable lead iodide perovskite phase via surface functionalization[J]. Nano Letters, 2017, 17(7): 4405-4414.

[70] Sokolikova M S, Mattevi C. Direct synthesis of metastable phases of 2D transition metal dichalcogenides [J]. Chemical Society Reviews, 2020, 49(12): 3952-3980.

[71] Singh A K, Zhou L, Shinde A, et al. Electrochemical stability of metastable materials [J]. Chemistry of Materials, 2017, 29(23): 10159-10167.

[72] Xiao J, Ouyang G, Liu P, et al. Reversible nanodiamond-carbon onion phase transformations [J]. Nano Letters, 2014, 14(6): 3645-3652.

[73] Liu P, Cao Y L, Wang C X, et al. Micro- and nanocubes of carbon with C_8-like and blue luminescence [J]. Nano Letters, 2008, 8(8): 2570-2575.

[74] Xiao J, Li J L, Liu P, et al. A new phase transformation path from nanodiamond to new-diamond via an intermediate carbon onion [J]. Nanoscale, 2014, 6(24): 15098-15106.

[75] Xiao J, Liu P, Liang Y, et al. Super-stable ultrafine beta-tungsten nanocrystals with metastable phase and related magnetism[J]. Nanoscale, 2013, 5(3): 899-903.

[76] Chen X Y, Cui H, Liu P, et al. Double-layer hexagonal Fe nanocrystals and magnetism [J]. Chemistry of Materials, 2008, 20(5): 2035-2038.

[77] Zeng Z D, Zeng Q S, Mao W L, et al. Phase transitions in metastable phases of silicon[J]. Journal of Applied Physics, 2014, 115(10): 103514.

[78] Liu P, Cao Y L, Chen X Y, et al. Trapping high-pressure nanophase of Ge upon laser ablation in liquid[J]. Crystal Growth & Design, 2009, 9(3): 1390-1393.

[79] Liu P, Cao Y L, Cui H, et al. Synthesis of GaN nanocrystals through phase transition from hexagonal to cubic structures upon laser ablation in liquid [J]. Crystal Growth & Design, 2008, 8(2): 559-563.

[80] Wang J B, Yang G W, Zhang C Y, et al. Cubic-BN nanocrystals synthesis by pulsed laser induced liquid-solid interfacial reaction [J]. Chemical Physics Letters, 2003, 367(1/2): 10-14.

[81] Yang G W, Wang J B. Carbon nitride nanocrystals having cubic structure using pulsed laser induced liquid-solid interfacial reaction[J]. Applied Physics A, 2000, 71(3): 343-344.

[82] Tan D Z, Lin G, Liu Y, et al. Synthesis of nanocrystalline cubic zirconia using femtosecond laser ablation[J]. Journal of Nanoparticle Research, 2011, 13(3): 1183-1190.

[83] Singh P, Kumar R, Singh R K. Progress on transition metal-doped ZnO nanoparticles and its application[J]. Industrial & Engineering Chemistry Research, 2019, 58(37): 17130-17163.

[84] Chen S, Huang D L, Xu P, et al. Semiconductor-based photocatalysts for photocatalytic and photoelectrochemical water splitting: Will we stop with photocorrosion? [J]. Journal of Materials Chemistry A, 2020, 8(5): 2286-2322.

[85] Zhu S S, Zhang P P, Chang L, et al. Photochemical fabrication of 3D hierarchical Mn_3O_4/H-TiO_2 composite films with excellent electrochemical capacitance performance [J]. Physical Chemistry Chemical Physics, 2016, 18(12): 8529-8536.

[86] Berr M, Vaneski A, Susha A S, et al. Colloidal CdS nanorods decorated with subnanometer sized Pt clusters for photocatalytic hydrogen generation[J]. Applied Physics Letters, 2010, 97(9): 093108.

[87] Peled A, Naddaka M, Lellouche J P. Controllable photodeposition of metal nanoparticles on a photoreactive silica support[J]. Journal of Materials Chemistry, 2012, 22(15): 7580-7853.

[88] Sun L L, Zhao D X, Song Z M, et al. Gold nanoparticles modified ZnO nanorods with improved photocatalytic activity [J]. Journal of Colloid and Interface Science, 2011, 363(1): 175-181.

[89] Ma J Q, Guo X H, Ge H G, et al. Seed-mediated photodeposition route to Ag-decorated SiO_2@TiO_2 microspheres with ideal core-shell structure and enhanced photocatalytic activity[J]. Applied Surface Science, 2018, 434: 1007-1014.

[90] Wang X W, Wang W Y, Miao Y Q, et al. Facet-selective photodeposition of gold nanoparticles on faceted ZnO crystals for visible light photocatalysis [J]. Journal of Colloid and Interface Science, 2016, 475: 112-118.

[91] Yang S K, Li M Y, Zhu X, et al. Photochemical synthesis of hierarchical multiple-growth-hillock superstructures of silver nanoparticles on ZnO [J]. The Journal of Physical Chemistry C, 2015, 119 (25): 14312-14318.

[92] Uma K, Arjun N, Pan G T, et al. The photodeposition of surface plasmon Ag metal on SiO_2@α-Fe_2O_3 nanocomposites sphere for enhancement of the photo-Fenton behavior [J]. Applied Surface Science, 2017, 425: 377-383.

[93] Zhou N, Ye C, Polavarapu L, et al. Controlled preparation of Au/Ag/SnO_2 core-shell nanoparticles using a photochemical method and applications in LSPR based sensing[J]. Nanoscale, 2015, 7(19): 9025-9032.

[94] Read C G, Steinmiller E M P, Choi K S. Atomic plane-selective deposition of gold nanoparticles on metal oxide crystals exploiting preferential adsorption of additives[J]. Journal of the American Chemical Society, 2009, 131(34): 12040-12041.

[95] Zhang F X, Chen J X, Zhang X, et al. Synthesis of titania-supported platinum catalyst: The effect of pH on morphology control and valence state during photodeposition [J]. Langmuir, 2004, 20(21): 9329-9334.

[96] Choi D, Jang D J. Photodeposition of gold nanoparticles on silica nanospheres using carbon dots as excellent electron donors [J]. New Journal of Chemistry, 2018, 42(18): 14717-14720.

[97] Xu L L, Zhang H, Tian Y, et al. Photochemical synthesis of ZnO@Au nanorods as an advanced reusable SERS substrate for ultrasensitive detection of light-resistant organic pollutant in wastewater[J]. Talanta, 2019, 194: 680-688.

[98] Xu L L, Li S, Li F, et al. Ultraviolet light-induced photochemical reaction for controlled fabrication of Ag nano-Islands on ZnO nanosheets: An advanced inexpensive substrate for ultrasensitive surface-enhanced Raman scattering analysis [J]. Optical Materials Express, 2017, 7(9): 3137-3146.

[99] de Corrado J M, Fernando J F S, Shortell M P, et al. ZnO colloid crystal facet-type determines both Au photodeposition and photocatalytic activity [J]. ACS Applied Nano Materials, 2019, 2(12): 7856-7869.

[100] Zhang X F, Wang Z G, Zhong Y X, et al. TiO_2 nanorods loaded with AuPt alloy nanoparticles for the photocatalytic oxidation of benzyl alcohol [J]. Journal of Physics and Chemistry of Solids, 2019, 126: 27-32.

[101] Klein M, Nadolna J, Gołąbiewska A, et al. The effect of metal cluster deposition route on structure and photocatalytic activity of mono- and bimetallic nanoparticles supported on TiO_2 by radiolytic method [J]. Applied Surface Science, 2016, 378: 37-48.

[102] Bhardwaj S, Pal B. Photodeposition of Ag and Cu binary co-catalyst onto TiO_2 for improved optical and photocatalytic degradation properties [J]. Advanced Powder Technology, 2018, 29(9): 2119-2128.

[103] Haselmann G M, Baumgartner B, Wang J, et al. *In situ* Pt photodeposition and methanol photooxidation on Pt/TiO_2: Pt-loading-dependent photocatalytic reaction pathways studied by liquid-phase infrared spectroscopy[J]. ACS Catalysis, 2020, 10(5): 2964-2977.

[104] Yamamoto M, Minoura Y, Akatsuka M, et al. Comparison of platinum photodeposition processes on two types of titanium dioxide photocatalysts[J]. Physical Chemistry Chemical Physics, 2020, 22(16): 8730-8738.

[105] Singh J, Sahu K, Pandey A, et al. Atom beam sputtered Ag-TiO_2 plasmonic nanocomposite thin films for photocatalytic applications [J]. Applied Surface Science, 2017, 411: 347-354.

[106] Georgakilas V, Otyepka M, Bourlinos A B, et al. Functionalization of graphene: Covalent and non-covalent approaches, derivatives and applications [J]. Chemical Reviews, 2012, 112(11): 6156-6214.

[107] Gao C, Guo Z, Liu J H, et al. The new age of carbon nanotubes: An updated review of functionalized carbon nanotubes in electrochemical sensors[J]. Nanoscale, 2012, 4(6): 1948-1963.

[108] Lin Y, Connell J W. Advances in 2D boron nitride nanostructures: Nanosheets, nanoribbons, nanomeshes, and hybrids with graphene[J]. Nanoscale, 2012, 4(22): 6908-6939.

[109] Yin F, Gu B B, Lin Y N, et al. Functionalized 2D nanomaterials for gene delivery applications [J]. Coordination Chemistry Reviews, 2017, 347: 77-97.

[110] Wang X W, Cheng L. Multifunctional two-dimensional nanocomposites for photothermal-based combined cancer therapy[J]. Nanoscale, 2019, 11(34): 15685-15708.

[111] Wu L Y, Wu K, Lei C X, et al. Surface modifications of boron nitride nanosheets for poly(vinylidene fluoride) based film capacitors: Advantages of edge-hydroxylation [J]. Journal of Materials Chemistry A, 2019, 7(13): 7664-7674.

[112] Chettri P, Vendamani V S, Tripathi A, et al. Green synthesis of silver nanoparticle-reduced graphene oxide using Psidium guajava and its application in SERS for the detection of methylene blue[J]. Applied Surface Science, 2017, 406: 312-318.

[113] Fan Z, Kanchanapally R, Ray P C. Hybrid graphene oxide based ultrasensitive SERS probe for label-free biosensing [J]. The Journal of Physical Chemistry Letters, 2013, 4(21): 3813-3818.

[114] Lai H S, Xu F G, Zhang Y, et al. Recent progress on graphene-based substrates for surface-enhanced Raman scattering applications [J]. Journal of Materials Chemistry B, 2018, 6(24): 4008-4028.

[115] Tian Y, Zhang H, Xu L L, et al. An additional electron-phonon coupling enhancement for improving SERS activity by supporting core-shell Au@Ag particles on carbon nanotubes[J]. Applied Physics Letters, 2019, 115(10): 101901.

[116] Xu L L, Zhang H, Tian Y, et al. Modified photochemical strategy to support highly-purity, dense and monodisperse Au nanospheres on graphene oxide for optimizing SERS detection[J]. Talanta, 2020, 209: 120535.

[117] Zhang Y C, He S, Guo W X, et al. Surface-plasmon-driven hot electron photochemistry [J]. Chemical Reviews, 2018, 118(6): 2927-2954.

[118] Zhang J, Li S Z, Wu J S, et al. Plasmon-mediated synthesis of silver triangular bipyramids [J]. Angewandte Chemie International Edition, 2009, 48(42): 7787-7791.

[119] Tang B, Xu S P, An J, et al. Photoinduced shape conversion and reconstruction of silver nanoprisms [J]. The Journal of Physical Chemistry C, 2009, 113(17): 7025-7030.

[120] Personick M L, Langille M R, Zhang J, et al. Plasmon-mediated synthesis of silver cubes with unusual twinning structures using short wavelength excitation[J]. Small, 2013, 9(11): 1947-1953.

[121] Pietrobon B, Kitaev V. Photochemical synthesis of monodisperse size-controlled silver decahedral nanoparticles and their remarkable optical properties [J]. Chemistry of Materials, 2008, 20(16): 5186-5190.

[122] Xue C, Métraux G S, Millstone J E, et al. Mechanistic study of photomediated triangular silver nanoprism growth [J]. Journal of the American Chemical Society, 2008, 130(26): 8337-8344.

[123] Zhang J, Langille M R, Mirkin C A. Synthesis of silver nanorods by low energy excitation of spherical plasmonic seeds[J]. Nano Letters, 2011, 11(6): 2495-2498.

[124] Brus L. Plasmon-driven chemical synthesis: Growing gold nanoprisms with light [J]. Nature Materials, 2016, 15(8): 824-825.

[125] Jin R, Cao Y, Mirkin C A, et al. Photoinduced conversion of silver nanospheres to nanoprisms[J]. Science, 2001, 294(5548): 1901-1903.

[126] Zhai Y, DuChene J S, Wang Y C, et al. Polyvinylpyrrolidone-induced anisotropic growth of gold nanoprisms in plasmon-driven synthesis [J]. Nature Materials, 2016, 15(8): 889-895.

[127] Xu L L, Li S, Zhang H, et al. Laser-induced photochemical synthesis of branched Ag@Au bimetallic nanodendrites as a prominent substrate for surface-enhanced Raman scattering spectroscopy[J]. Optics Express, 2017, 25(7): 7408-7417.

[128] Langille M R, Zhang J, Mirkin C A. Plasmon-mediated synthesis of heterometallic nanorods and icosahedra [J]. Angewandte Chemie International Edition, 2011, 50(15): 3543-3547.

[129] Qiu J J, Richey N E, DuChene J S, et al. Surface plasmon-mediated chemical solution deposition of Cu nanoparticle films[J]. The Journal of Physical Chemistry C, 2016, 120(37): 20775-20780.

[130] Forcherio G T, Baker D R, Boltersdorf J, et al. Targeted deposition of platinum onto gold nanorods by plasmonic hot electrons [J]. The Journal of Physical Chemistry C, 2018, 122(50): 28901-28909.

[131] Habib A, King M E, Etemad L L, et al. Plasmon-mediated synthesis of hybrid silver-platinum nanostructures [J]. The Journal of Physical Chemistry C, 2020, 124(12): 6853-6860.

[132] Langer J, de Jimenez Aberasturi D, Aizpurua J, et al. Present and future of surface-enhanced Raman scattering[J]. ACS Nano, 2020, 14(1): 28-117.

[133] He J, Qiao Y, Zhang H B, et al. Gold-silver nanoshells promote wound healing from drug-resistant bacteria infection and enable monitoring via surface-enhanced Raman scattering imaging [J]. Biomaterials, 2020, 234: 119763.

[134] Chen Y S, Zhang Y X, Pan F, et al. Breath analysis based on surface-enhanced Raman scattering sensors distinguishes early and advanced gastric cancer patients from healthy persons [J]. ACS Nano, 2016, 10(9): 8169-8179.

[135] Wei W, Du Y X, Zhang L M, et al. Improving SERS hot spots for on-site pesticide detection by combining silver nanoparticles with nanowires[J]. Journal of Materials Chemistry C, 2018, 6(32): 8793-8803.

[136] Hao N Y, Chen M, Yang H, et al. "pomegranate-like" plasmonic nanoreactors with accessible high-density hotspots for *in situ* SERS monitoring of catalytic reactions[J]. Analytical Chemistry, 2020, 92(5): 4115-4122.

[137] Zhou Z F, Lu J L, Wang J Y, et al. Trace detection of polycyclic aromatic hydrocarbons in environmental waters by SERS [J]. Spectrochimica Acta Part A:

Molecular and Biomolecular Spectroscopy, 2020, 234: 118250.

[138] Li H Z, Yang Q, Hou J, et al. Bioinspired micropatterned superhydrophilic Au-areoles for surface-enhanced Raman scattering (SERS) trace detection [J]. Advanced Functional Materials, 2018, 28(21): 1800448.

[139] Zong C, Xu M X, Xu L J, et al. Surface-enhanced Raman spectroscopy for bioanalysis: Reliability and challenges[J]. Chemical Reviews, 2018, 118(10): 4946-4980.

[140] Yaseen T, Pu H B, Sun D W. Functionalization techniques for improving SERS substrates and their applications in food safety evaluation: A review of recent research trends[J]. Trends in Food Science & Technology, 2018, 72: 162-174.

[141] Radziuk D, Moehwald H. Prospects for plasmonic hot spots in single molecule SERS towards the chemical imaging of live cells[J]. Physical Chemistry Chemical Physics, 2015, 17(33): 21072-21093.

[142] Zrimsek A B, Wong N L, van Duyne R P. Single molecule surface-enhanced Raman spectroscopy: A critical analysis of the bianalyte versus isotopologue proof[J]. The Journal of Physical Chemistry C, 2016, 120(9): 5133-5142.

[143] Zrimsek A B, Chiang N H, Mattei M, et al. Single-molecule chemistry with surface- and tip-enhanced Raman spectroscopy[J]. Chemical Reviews, 2017, 117(11): 7583-7613.

[144] dos Santos D, Temperini M L A, Brolo A G. Intensity fluctuations in single-molecule surface-enhanced Raman scattering[J]. Accounts of Chemical Research, 2019, 52(2): 456-464.

[145] Choi H K, Lee K S, Shin H H, et al. Single-molecule surface-enhanced Raman scattering as a probe of single-molecule surface reactions: Promises and current challenges [J]. Accounts of Chemical Research, 2019, 52(11): 3008-3017.

[146] Sigle D O, Kasera S, Herrmann L O, et al. Observing single molecules complexing with cucurbit[7]uril through nanogap surface-enhanced Raman spectroscopy [J]. The Journal of Physical Chemistry Letters, 2016, 7(4): 704-710.

[147] Chen X J, Cabello G, Wu D Y, et al. Surface-enhanced Raman spectroscopy toward application in plasmonic photocatalysis on metal nanostructures [J]. Journal of Photochemistry and Photobiology C: Photochemistry Reviews, 2014, 21: 54-80.

[148] Song D, Yang R, Long F, et al. Applications of magnetic nanoparticles in surface-enhanced Raman scattering (SERS) detection of environmental pollutants[J]. Journal of Environmental Sciences, 2019, 80: 14-34.

[149] Cheng L, Ma C S, Yang G, et al. Hierarchical silver mesoparticles with tunable surface topographies for highly sensitive surface-enhanced Raman spectroscopy [J]. Journal of Materials Chemistry A, 2014, 2(13): 4534-4542.

[150] Jiang H Z, Xu D P, Kang W G, et al. Fractal study and SERS effect of silver nanowires with high surface roughness[J]. Acta Optica Sinica, 2019, 39(7): 0716001.
江恒泽, 徐大鹏, 康维刚, 等. 高表面粗糙度银纳米线的分形研究和SERS效应[J]. 光学学报, 2019, 39(7): 0716001.

[151] Liu K, Bai Y C, Zhang L, et al. Porous Au-Ag nanospheres with high-density and highly accessible hotspots for SERS analysis [J]. Nano Letters, 2016, 16(6): 3675-3681.

[152] Zhang T, Zhou F, Hang L F, et al. Controlled synthesis of sponge-like porous Au-Ag alloy nanocubes for surface-enhanced Raman scattering properties [J]. Journal of Materials Chemistry C, 2017, 5(42): 11039-11045.

[153] Sun Y D, Li T. Composition-tunable hollow Au/Ag SERS nanoprobes coupled with target-catalyzed hairpin assembly for triple-amplification detection of miRNA[J]. Analytical Chemistry, 2018, 90(19): 11614-11621.

[154] Dai L W, Song L P, Huang Y J, et al. Bimetallic Au/Ag core-shell superstructures with tunable surface plasmon resonance in the near-infrared region and high performance surface-enhanced Raman scattering[J]. Langmuir, 2017, 33(22): 5378-5384.

[155] Zhang T, Sun Y Q, Hang L F, et al. Periodic porous alloyed Au-Ag nanosphere arrays and their highly sensitive SERS performance with good reproducibility and high density of hotspots[J]. ACS Applied Materials & Interfaces, 2018, 10(11): 9792-9801.

[156] Jiang X, Sun X D, Yin D, et al. Recyclable Au-TiO_2 nanocomposite SERS-active substrates contributed by synergistic charge-transfer effect[J]. Physical Chemistry Chemical Physics, 2017, 19(18): 11212-11219.

[157] Huang J, Ma D Y, Chen F, et al. Green *in situ* synthesis of clean 3D chestnutlike Ag/WO_{3-x} nanostructures for highly efficient, recyclable and sensitive SERS sensing[J]. ACS Applied Materials & Interfaces, 2017, 9(8): 7436-7446.

[158] Lai Y C, Ho H C, Shih B W, et al. High performance and reusable SERS substrates using Ag/ZnO heterostructure on periodic silicon nanotube substrate[J]. Applied Surface Science, 2018, 439: 852-858.

[159] Zhai Y, Zheng Y S, Ma Z Y, et al. Synergistic enhancement effect for boosting Raman detection sensitivity of antibiotics[J]. ACS Sensors, 2019, 4(11): 2958-2965.

[160] Ji S D, Kou S, Wang M Q, et al. Two-step synthesis of hierarchical Ag/Cu_2O/ITO substrate for ultrasensitive and recyclable surface-enhanced Raman spectroscopy applications [J]. Applied Surface Science, 2019, 489: 1002-1009.

[161] Liu H, Wei L, Hua J H, et al. Enzyme activity-modulated etching of gold nanobipyramids@MnO_2 nanoparticles for ALP assay using surface-enhanced Raman spectroscopy[J]. Nanoscale, 2020, 12(18): 10390-10398.

[162] Tao G Q, Wang J. Gold nanorod@nanoparticle seed-SERSnanotags/graphene oxide plasmonic superstructured nanocomposities as an "on-off" SERS aptasensor[J]. Carbon, 2018, 133: 209-217.

[163] Zhang C Y, Hao R, Zhao B, et al. A ternary functional Ag@GO@Au sandwiched hybrid as an ultrasensitive and stable surface enhanced Raman scattering platform [J]. Applied Surface Science, 2017, 409: 306-313.

[164] Zeng F Y, Xu D D, Zhan C, et al. Surfactant-free synthesis of graphene oxide coated silver nanoparticles for SERS biosensing and intracellular drug delivery [J]. ACS Applied Nano Materials, 2018, 1(6): 2748-2753.

[165] Li J Y, Heng H, Lü J, et al. Graphene oxide-assisted and DNA-modulated SERS of AuCu alloy for the fabrication of apurinic/apyrimidinic endonuclease 1 biosensor[J]. Small, 2019, 15(48): 1901506.

[166] Dizajghorbani-Aghdam H, Miller T S, Malekfar R, et al. SERS-active Cu nanoparticles on carbon nitride support fabricated using pulsed laser ablation [J]. Nanomaterials, 2019, 9(9): 1223.

[167] Wang X T, Shi W X, Jin Z, et al. Remarkable SERS activity observed from amorphous ZnO nanocages [J]. Angewandte Chemie International Edition, 2017, 56(33): 9851-9855.

[168] Yang L B, Yin D, Shen Y, et al. Mesoporous semiconducting TiO_2 with rich active sites as a remarkable substrate for surface-enhanced Raman scattering [J]. Physical Chemistry Chemical Physics, 2017, 19(28): 18731-18738.

[169] Lin J, Shang Y, Li X X, et al. Ultrasensitive SERS detection by defect engineering on single Cu_2O superstructure particle [J]. Advanced Materials, 2017, 29(5): 1604797.

[170] Han X X, Ji W, Zhao B, et al. Semiconductor-enhanced Raman scattering: Active nanomaterials and applications[J]. Nanoscale, 2017, 9(15): 4847-4861.

[171] Hou H, Wang P, Zhang J, et al. Graphene oxide-supported Ag nanoplates as LSPR tunable and reproducible substrates for SERS applications with optimized sensitivity[J]. ACS Applied Materials & Interfaces, 2015, 7(32): 18038-18045.

[172] Li Z, Jiang S Z, Huo Y Y, et al. 3D silver nanoparticles with multilayer graphene oxide as a spacer for surface enhanced Raman spectroscopy analysis[J]. Nanoscale, 2018, 10(13): 5897-5905.

[173] Ding G H, Xie S, Liu Y, et al. Graphene oxide-silver nanocomposite as SERS substrate for dye detection: Effects of silver loading amount and composite dosage [J]. Applied Surface Science, 2015, 345: 310-318.

[174] Jiang Y, Wang J, Malfatti L, et al. Highly durable graphene-mediated surface enhanced Raman scattering (G-SERS) nanocomposites for molecular detection[J]. Applied Surface Science, 2018, 450: 451-460.

[175] Alamri M, Sakidja R, Goul R, et al. Plasmonic Au nanoparticles on 2D MoS_2/graphene van der waals heterostructures for high-sensitivity surface-enhanced Raman spectroscopy[J]. ACS Applied Nano Materials, 2019, 2(3): 1412-1420.

[176] Zhang N, Tong L M, Zhang J. Graphene-based enhanced Raman scattering toward analytical applications[J]. Chemistry of Materials, 2016, 28(18): 6426-6435.

[177] Tan Y, Ma L N, Gao Z B, et al. Two-dimensional heterostructure as a platform for surface-enhanced Raman scattering[J]. Nano Letters, 2017, 17(4): 2621-2626.

[178] Wang Z Q, Wu S S, Colombi Ciacchi L, et al.

Graphene-based nanoplatforms for surface-enhanced Raman scattering sensing[J]. The Analyst, 2018, 143(21): 5074-5089.

[179] Zhang H, Li G H, Li S, et al. Boron nitride/gold nanocomposites for crystal violet and creatinine detection by surface-enhanced Raman spectroscopy [J]. Applied Surface Science, 2018, 457: 684-694.

[180] Zhang H, Cui Q Q, Xu L L, et al. Blue laser-induced photochemical synthesis of CuAg nanoalloys on h-BN supports with enhanced SERS activity for trace-detection of residual pesticides on tomatoes[J]. Journal of Alloys and Compounds, 2020, 825: 153996.

[181] Chen D Y, Li B L, Pu Q M, et al. Preparation of Ag-AgVO$_3$/g-C3N4 composite photo-catalyst and degradation characteristics of antibiotics[J]. Journal of Hazardous Materials, 2019, 373: 303-312.

[182] Zhang H B, Zhang P, Qiu M, et al. Ultrasmall MoO$_x$ clusters as a novel cocatalyst for photocatalytic hydrogen evolution [J]. Advanced Materials, 2019, 31(6): 1804883.

[183] Wang P, Wu Y H, Cai B, et al. Solution-processable perovskite solar cells toward commercialization: Progress and challenges [J]. Advanced Functional Materials, 2019, 29(47): 1807661.

[184] Li A, Wang T, Li C C, et al. Adjusting the reduction potential of electrons by quantum confinement for selective photoreduction of CO_2 to methanol [J]. Angewandte Chemie International Edition, 2019, 58 (12): 3804-3808.

[185] Li A, Zhu W J, Li C C, et al. Rational design of yolk-shell nanostructures for photocatalysis [J]. Chemical Society Reviews, 2019, 48(7): 1874-1907.

[186] Yang X G, Wang D W. Photocatalysis: from fundamental principles to materials and applications [J]. ACS Applied Energy Materials, 2018, 1(12): 6657-6693.

[187] Liu L Q, Zhang X N, Yang L F, et al. Metal nanoparticles induced photocatalysis [J]. National Science Review, 2017, 4(5): 761-780.

[188] Hao R G, Kong X P, Zhao Z, et al. *In-situ* electrochemical-photoreduction synthesis and photocatalytic performance of Pd/BiF$_3$ thin films[J]. Acta Optica Sinica, 2020, 40(18): 1831001.
郝瑞刚, 孔祥鹏, 赵祖, 等. 原位电化学-光还原法制备 Pd/BiF$_3$薄膜及其光催化性能[J]. 光学学报, 2020, 40 (18): 1831001.

[189] Zhang Z L, Zhang C Y, Zheng H R, et al. Plasmon-driven catalysis on molecules and nanomaterials[J]. Accounts of Chemical Research, 2019, 52 (9): 2506-2515.

[190] Waiskopf N, Ben-Shahar Y, Banin U. Photocatalytic hybrid semiconductor-metal nanoparticles: from synergistic properties to emerging applications[J]. Advanced Materials, 2018, 30(41): 1706697.

[191] Gao W Q, Liu Q L, Zhang S, et al. Electromagnetic induction derived micro-electric potential in metal-semiconductor core-shell hybrid nanostructure enhancing charge separation for high performance photocatalysis[J]. Nano Energy, 2020, 71: 104624.

[192] Li J Y, Yan P, Li K L, et al. Cu supported on polymeric carbon nitride for selective CO_2 reduction into CH_4: A combined kinetics and thermodynamics investigation[J]. Journal of Materials Chemistry A, 2019, 7(28): 17014-17021.

[193] Hu J Y, Zhang S S, Cao Y H, et al. Novel highly active anatase/rutile TiO_2 photocatalyst with hydrogenated heterophase interface structures for photoelectrochemical water splitting into hydrogen [J]. ACS Sustainable Chemistry & Engineering, 2018, 6(8): 10823-10832.

[194] Yan B X, Wang Y C, Jiang X Y, et al. Flexible photocatalytic composite film of ZnO-microrods/polypyrrole[J]. ACS Applied Materials & Interfaces, 2017, 9(34): 29113-29119.

[195] Liu Y, Ma Y J, Liu W W, et al. Facet and morphology dependent photocatalytic hydrogen evolution with CdS nanoflowers using a novel mixed solvothermal strategy[J]. Journal of Colloid and Interface Science, 2018, 513: 222-230.

[196] Dong P Y, Hou G H, Xi X G, et al. WO_3-based photocatalysts: Morphology control, activity enhancement and multifunctional applications[J]. Environmental Science: Nano, 2017, 4(3): 539-557.

[197] Zhang L P, Ran J R, Qiao S Z, et al. Characterization of semiconductor photocatalysts [J]. Chemical Society Reviews, 2019, 48 (20): 5184-5206.

[198] Zeng H B, Cai W P, Liu P S, et al. ZnO-based hollow nanoparticles by selective etching: Elimination and reconstruction of metal-semiconductor interface, improvement of blue emission and photocatalysis [J]. ACS Nano, 2008, 2(8): 1661-1670.

[199] Zeng H B, Liu P S, Cai W P, et al. Controllable Pt/ZnO porous nanocages with improved photocatalytic activity [J]. The Journal of Physical

Chemistry C, 2008, 112(49): 19620-19624.

[200] Wang Z W, Wang Z Y, Wang D M, et al. Ultra-small Sn_2S_3 porous nano-particles: An excellent photo-catalyst in the reduction of aqueous Cr(VI) under visible light irradiation[J]. RSC Advances, 2016, 6(15): 12286-12289.

[201] Li Q, Liang C H, Tian Z F, et al. Core-shell Ta_xO@Ta_2O_5 structured nanoparticles: Laser ablation synthesis in liquid, structure and photocatalytic property [J]. CrystEngComm, 2012, 14(9): 3236-3240.

[202] Zhang H M, Liang C H, Tian Z F, et al. Hydrothermal treatment of colloids induced via liquid-phase laser ablation: A new approach for hierarchical titanate nanostructures with enhanced photodegradation performance[J]. CrystEngComm, 2011, 13(14): 4676-4682.

[203] Cai Y Y, Ye Y X, Tian Z F, et al. *In situ* growth of lamellar $ZnTiO_3$ nanosheets on TiO_2 tubular array with enhanced photocatalytic activity[J]. Physical Chemistry Chemical Physics, 2013, 15(46): 20203-20209.

[204] Lin Z Y, Liu P, Yan J H, et al. Matching energy levels between TiO_2 and α-Fe_2O_3 in a core-shell nanoparticle for visible-light photocatalysis [J]. Journal of Materials Chemistry A, 2015, 3(28): 14853-14863.

[205] Lin Z Y, Xiao J, Yan J H, et al. Ag/AgCl plasmonic cubes with ultrahigh activity as advanced visible-light photocatalysts for photodegrading dyes [J]. Journal of Materials Chemistry A, 2015, 3(14): 7649-7658.

[206] Lin Z Y, Li J L, Zheng Z Q, et al. Electronic reconstruction of α-Ag_2WO_4 Nanorods for visible-light photocatalysis[J]. ACS Nano, 2015, 9(7): 7256-7265.

[207] Staude I, Miroshnichenko A E, Decker M, et al. Tailoring directional scattering through magnetic and electric resonances in subwavelength silicon nanodisks[J]. ACS Nano, 2013, 7(9): 7824-7832.

[208] Wu S L, Wang P P, Cai Y Y, et al. Reduced graphene oxide anchored magnetic $ZnFe_2O_4$ nanoparticles with enhanced visible-light photocatalytic activity[J]. RSC Advances, 2015, 5(12): 9069-9074.

[209] Park H, Reddy D A, Kim Y, et al. Synthesis of ultra-small palladium nanoparticles deposited on CdS nanorods by pulsed laser ablation in liquid: Role of metal nanocrystal size in the photocatalytic hydrogen production[J]. Chemistry - A European Journal, 2017, 23(53): 13112-13119.

[210] Liao L, Zhang Q H, Su Z H, et al. Efficient solar water-splitting using a nanocrystalline CoO photocatalyst[J]. Nature Nanotechnology, 2014, 9(1): 69-73.

[211] Lin Z Y, Xiao J, Li L H, et al. Nanodiamond-embedded p-type copper(I) oxide nanocrystals for broad-spectrum photocatalytic hydrogen evolution [J]. Advanced Energy Materials, 2016, 6(4): 1501865.

[212] Guo W, Liu B. Liquid-phase pulsed laser ablation and electrophoretic deposition for chalcopyrite thin-film solar cell application [J]. ACS Applied Materials & Interfaces, 2012, 4(12): 7036-7042.

[213] Wang Z Y, Zhang H, Xu L L, et al. Laser-induced fabrication of highly branched Au@TiO_2 nano-dendrites with excellent near-infrared absorption properties [J]. RSC Advances, 2016, 6(86): 83337-83342.

[214] Yang R Y, Zhang Z Y, Xu L L, et al. Laser-induced fabrication of highly branched CuS nanocrystals with excellent near-infrared absorption properties [J]. Chinese Physics B, 2017, 26(6): 076102.

[215] Yu Y, Yan L H, Si J H, et al. Femtosecond laser assisted synthesis of gold nanorod and graphene hybrids and its photothermal property in the near-infrared region[J]. Journal of Physics and Chemistry of Solids, 2019, 132: 116-120.

[216] Ma C, Yan J, Huang Y, et al. The optical duality of tellurium nanoparticles for broadband solar energy harvesting and efficient photothermal conversion[J]. Science Advances, 2018, 4(8): eaas9894.